

THE CANONICAL WNT SIGNALING PATHWAY AFFECTS REGENERATION OF
MECHANOSENSORY HAIR CELLS IN *DANIO RERIO*

A THESIS IN
Cellular and Molecular Biology

Presented to the Faculty of the University of
Missouri-Kansas City in partial fulfillment of
the requirements for the degree

MASTER OF SCIENCE

By

ELLEN MEGERSON

B.S., University of Denver, 2018

Kansas City, Missouri

2020

THE CANONICAL WNT SIGNALING PATHWAY AFFECTS REGENERATION OF
MECHANOSENSORY HAIR CELLS IN *DANIO RERIO*

Ellen Megerson, Candidate for the Master of Science Degree

University of Missouri-Kansas City, 2020

ABSTRACT

In vertebrates, mechanosensory hair cells are located in the inner ear and mediate hearing. When damage to these specialized cells occur, it leads to irreversible hearing loss. Not only do aquatic vertebrates have inner ear hair cells, but mechanosensory hair cells are also found in the lateral line system. The lateral line system senses variation in water current. Neuromast mechanosensory organs comprise the lateral line and consist of hair cells, supporting cells and mantle cells. In zebrafish, hair cells of the lateral line have demonstrated a robust ability to regenerate following damage.

Previous studies have suggested that hair cells are replaced via the division and differentiation of their surrounding support cells. Research using pharmacological modulators of the Wnt pathway has suggested that the Wnt pathway potentially plays a role in lateral line hair cell regeneration. In this current study, we examine the role of the Wnt signaling pathway in hair cell regeneration by employing Wnt pathway mutant zebrafish lines.

Mutations in LRP5, Lef1 and a negative regulator of Wnt signaling, Kremen1, were used to study the role of Wnt signaling in regeneration of lateral line hair cells in zebrafish. These Wnt pathway mutant lines show no change in proliferation of supporting cells post injury and

shifts in the number of regenerated hair cells. The results obtained in this study suggest that disrupting Wnt signaling at distinct points along the pathway leads to differential patterns of hair cell regeneration, including specification of dividing support cells. Understanding the role of the Wnt signaling pathway in zebrafish mutants will contribute to subsequent studies on hearing loss reversal in mammals with inner ear hair cell damage.

APPROVAL PAGE

The faculty listed below, appointed by the Dean of the School of Biological and Chemical Sciences, have examined a thesis title “The Canonical Wnt Signaling Pathway Affects Regeneration of Mechanosensory Hair Cells in *Danio rerio*”, presented by Ellen Megerson, candidate for the Master of Science degree and certify that in their opinion it is worthy of acceptance.

Supervisory Committee

Hillary McGraw, Ph.D
Department of Genetics, Developmental and Evolutionary Biology

Samuel Bouyain, Ph.D
Department of Cell and Molecular Biology and Biochemistry

Stephane Dissel, Ph.D
Department of Genetics, Developmental and Evolutionary

CONTENTS

ABSTRACT	iii
LIST OF ILLUSTRATIONS	viii
LIST OF TABLES	ix
ACKNOWLEDGEMENTS	x
Chapter	
1. INTRODUCTION	1
1.1 Structure and function of hair cells	1
1.2 The lateral line mechanosensory system	4
1.3 Regeneration	6
1.4 Wnt signaling pathway	9
1.5 Present study	12
2. MATERIALS AND METHODS	15
2.1 Staining for all hair cells and functional hair cells in the neuromast	15
2.2 Identifying cellular proliferation in neuromasts	17
2.3 Treatment with AZK	19
2.4 Treatment with IWR	21
2.5 Data Collection and analysis	22
2.6 Imaging neuromasts using confocal microscopy	22
3. RESULTS	23
3.1 Introduction to results	23
3.2 Eight-day regeneration in <i>lef1^{n/2}</i> mutants	24
3.3 Cell proliferation in <i>lef1^{n/2}</i> mutant neuromasts	27

3.4 Eight-day regeneration in <i>krm1^{nl10}</i> mutants.....	28
3.5 Cell proliferation in <i>krm1^{nl10}</i> mutant neuromasts	32
3.6 Eight-day regeneration in <i>lrp5^{nl23}</i> mutants	34
3.7 Cell proliferation in <i>lrp5^{nl23}</i> mutant neuromasts.....	38
3.8 Eight day regeneration of AZK treated fish	40
3.9 Cell proliferation in AZK treated neuromasts	42
3.10 Eight day regeneration of IWR-1 treated fish	44
3.11 Proliferation in IWR-1 treated zebrafish	46
4. DISCUSSION.....	49
REFERENCE LIST	53
VITA.....	57

LIST OF ILLUSTRATION

Figure	Page
1.1 A mature hair cell	3
1.2 Anatomy of a neuromast	6
1.4 Wnt signaling pathway	11
1.5 Effects of AZK and IWR-1 on the Wnt signaling pathway	13
3.2A When the Lef1 transcription factor is not present, transcription of downstream target genes is not possible	24
3.2 Confocal images were taken of a <i>lef1^{1/2}</i> mutant and wildtype neuromast	26
3.3 Cellular proliferation in <i>lef1^{nl2}</i> homozygous and heterozygous siblings following regeneration	28
3.4A Null mutation of the Kremen1 co-receptor	30
3.4 Confocal images of <i>krm1nl10</i> homozygous and heterozygous neuromasts following regeneration	32
3.5 Cellular proliferation in a <i>krm1^{nl10}</i> homozygous and heterozygous Neuromast.....	34
3.6A <i>lrp5^{nl23}</i> null mutation	36
3.6 Confocal images were taken of a <i>lrp5^{nl23}</i> homozygous and heterozygous neuromast following regeneration	38
3.7 Cellular proliferation in a <i>lrp5^{nl23}</i> homozygous and heterozygous neuromast	40
3.8 Confocal images of AZK and DMSO treated fish following regeneration.....	42
3.9 Cellular proliferation in AZK and DMSO treated neuromasts	44

3.10	Confocal images of IWR-1 and DMSO treated fish following regeneration.....	46
3.11	Cellular proliferation in IWR-1 and DMSO treated neuromast	48

LIST OF TABLES

Table		Page
2.1	FM1-43 and anti-parvalbumin staining protocol.....	17
2.2	BrdU and DAPI staining protocol	19
2.3	AZK and DMSO treatment protocol.....	20
2.4	IWR-1 and DMSO treatment protocol	21

ACKNOWLEDGEMENTS

I would like to thank my committee chair and mentor, Dr. Hillary McGraw. She has been so incredibly helpful and encouraging during the project represented here in this thesis. I would also like to acknowledge my other thesis committee members, Dr. Bouyain and Dr. Dissel for all their advice concerning my thesis project. Finally, I would like to thank Anastasia Luna and Lauren Melton for their beneficial contributions to this project. I would also like to recognize Jaimie Johnson for his assistance with zebrafish husbandry.

CHAPTER 1

INTRODUCTION

1.1 Structure and function of hair cells

In 2012, it was reported that 14 percent (27.7 million) of American adults suffer from hearing loss (Hoffman et al., 2017). Hearing loss can be a result of damage to mechanosensory receptor cells termed hair cells, which are located in the inner ear (Olt et al., 2014). The destruction of hair cells may be induced by genetic, aging or environmental factors (Cramer et al., 2017). The vestibular system also relies on mechanosensory hair cells and destruction of these cells can result in vertigo or dizziness (Yoo and Mihaila, 2020). Hair cells in the adult mammalian inner ear and vestibular system do not regenerate following damage, rendering hearing loss and proprioception defects irreversible (Chai et al., 2012; Elkon et al., 2015). It is therefore of interest to expand on the current knowledge of hair cell regeneration.

The general structure of hair cells across sensory modalities includes stereocilia located at the apical surface which are organized asymmetrically based on increasing height. Stereocilia are formed thickly packed bulks of actin rather than microtubule as seen in typical cilia (Basu et al., 2016). Singular filaments located at the tip of stereocilia are called tip links and connect one stereocilia to the next (Nicolson, 2017). Tension is placed on tip links when changes in fluid movement in the inner ear or vestibular canals deflect the stereocilia towards the tallest stereocilia (Basu et al., 2016). This directional displacement results in the opening of mechanotransduction channels at the tips of the stereocilia allowing potassium to enter into the cell and elicit depolarization. Depolarization leads to a shift in membrane potential,

consequently resulting in neurotransmitter release onto the innervating afferent neuron (Nicolson, 2017).

There are two populations of hair cells in the cochlea of the mammal inner ears. The first group is called the inner hair cells, which release neurotransmitters from ribbon synapse in response to sound. The second group, the outer hair cells are critical for modulating sound-evoked vibrations (Fettiplace et al., 2017; Johnson et al., 2019). When the mechano-electrical transduction (MET) channel is opened during a depolarizing stimuli, neurotransmitters are released from the ribbon synapses located at the basal end of the hair cells. Neurotransmitters act upon the innervating afferent neuron, which carries the sensory signals to the brain (Johnson et al., 2019).

Damage to hair cells can be due to factors such as prolonged noise exposure. Several injuries to hair cells can occur, such as tip link damage. Tip links are critical for opening of the MET channels and when damaged, the hair cells do not have the ability to depolarize following stimulation. Previous studies have provided evidence that under specific conditions tip links have the ability to recover in vitro within 24 hours (Zhao et al., 1996). However, it is important to note that this repair is not due to the formation of new tip links via regeneration, but rather through the repair of the existing tip links. Mammals are unable to regenerate new hair cells following damage (Chai et al., 2012; Elkon et al., 2015).

Mechanosensory hair cells structurally analogous to inner ear hair cells are found in the lateral line of zebrafish (*Danio rerio*). The lateral line hair cells are of interest, as they demonstrate the robust ability to regenerate following damage (Ma et al., 2008; Dalle Nogare et al., 2017). This makes the zebrafish lateral line a prime model for understanding hair cell regeneration.

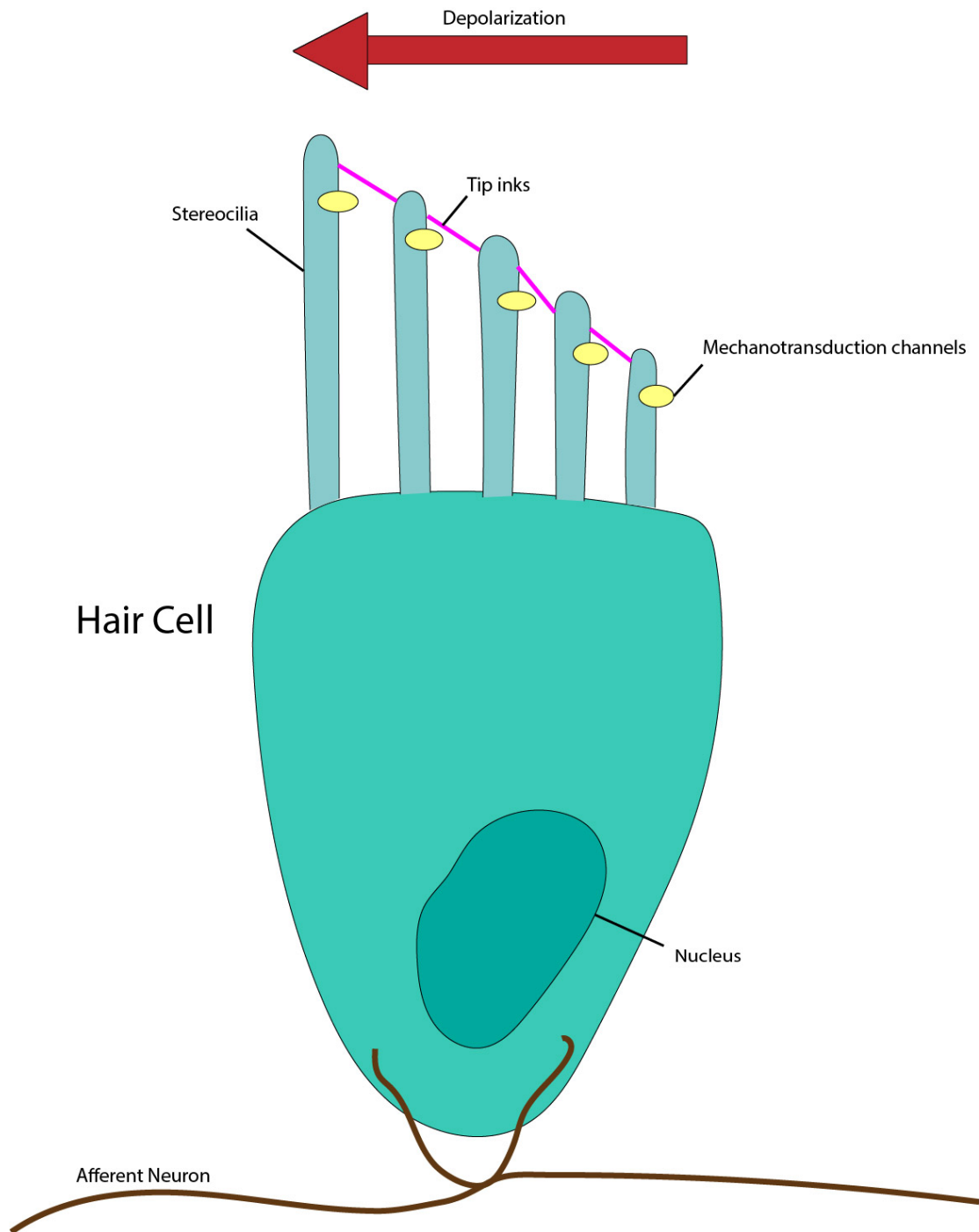


Figure 1.1. A mature hair cell. Mature hair cells contain stereocilia at the apical surface of the cell. Stereocilia house mechanotransduction channels near the tips. Tip links connect stereocilia and when stereocilia are deflected in a depolarizing direction, mechanotransduction channels are open. A hair cell is innervated by one afferent neuron which transmits information to the brain.

1.2 The lateral line mechanosensory system

The lateral line mechanosensory system is found in aquatic vertebrates, such as zebrafish (Dalle Nogare et al., 2017). It is a sensory system that detects hydrophonic stimuli, for instance water displacements and fluctuations in pressure (Bleckmann and Zelick, 2009). Swimming against current, prey detection and schooling are behaviors that rely on the lateral line (Ghysen and Dambly-Chaudiere, 2007). The lateral line is composed of clusters of epithelial cells known as neuromasts which are located on the body surface across the head and along the trunk (Dalle Nogare et al., 2017; Ghysen and Dambly-Chaudiere, 2007; Bleckmann and Zelick, 2009;).

There are two branches of the zebrafish lateral line, an anterior section that is located on the head and a posterior branch that spans from the trunk to the tail (Urasaki et al., 2019). The posterior lateral line is established via the migration of the posterior lateral line (pLL) primordium. The pLL primordium is a collection of approximately 100 cells that migrate caudally along the trunk between the skin and the developing muscle (Dalle Nogare et al., 2017).

The migration of the pLL primordium is guided by the chemokine Sdf1a, which is expressed in the underlying muscle precursor cells and interacts with the Cxcr4b and Cxcr7b receptors which are expressed in the primordium (Thomas et al., 2015). Migration begins around 20-22 hours post fertilization (hpf) and deposits 5-7 neuromasts and 2-3 terminal neuromasts by at the end of the tail 48 hpf. The rate of deposition of cells exceeds the rate of proliferation in the primordium, however the observed proliferation is able to maintain a relatively consistent size of the primordium. (Dalle Nogare et al., 2017). These deposits of

epithelial cells are called neuromasts and contain mechanosensory hair cells, support cells and mantle cells.

Hair cells are located centrally in the neuromast surrounded by supporting cells. Mantle cells are a quiescent stem cell population that are located around the outer edge of the neuromast (Kniss et al., 2016). These cells are only observed re-entering the cell cycle after serious harm to the sensory organ occurs (Romero-Carvajal et al., 2015). Unlike hair cells of the inner ear, zebrafish lateral line hair cells demonstrate the robust ability to regenerate following assault (Ma et al., 2008). The easy accessibility and the ability to regenerate makes the zebrafish lateral line hair cells a prime model for understanding hair cell regeneration.

Similar to intestinal and hair follicle stem cells, support cells are multipotent (Romero-Carvajal et al., 2015). Throughout the lifetime of zebrafish, dying hair cells are replenished by surrounding support cells. A previous study used time-lapse analyses of homeostatic and regenerating neuromasts to determine the patterns of support cell divisions and differentiation. The fate of each dividing cell was recorded leading to the conclusion that support cells are self-renewing stem cells (Lush et al., 2019)

Three populations of support cells have been identified in the neuromasts, based on cellular behavior and molecular markers (Thomas and Raible, 2019). The first are self-renewing cells that are located near the peripheral mantle cells along the dorsal-ventral poles. The second population of support cells are located at the anterior-posterior poles and in the center of the neuromast. These cells proliferate and differentiate. The final population only respond to extreme damage and are called quiescent peripheral mantle cells (Romero-Carvajal et al., 2015).

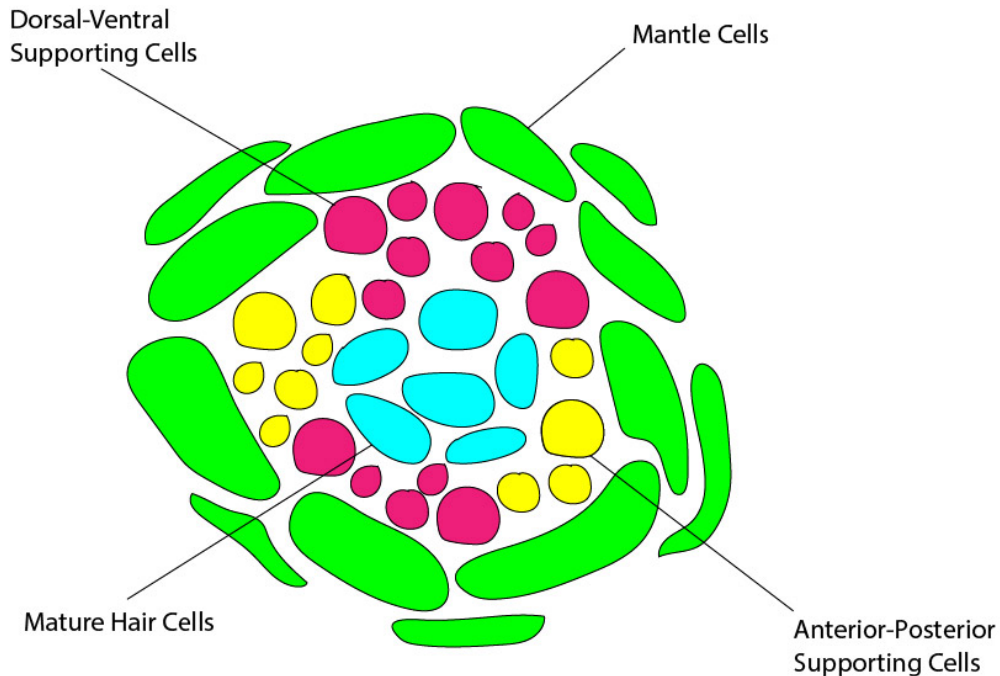


Figure 1.2. Anatomy of a neuromast. Neuromasts contain hair cells, supporting cells and mantle cells. Mantle cells are highlighted in green, dorsal-ventral supporting cells are shown in pink, anterior-posterior supporting cells are colored yellow and mature hair cells are detailed in cyan.

1.3 Regeneration

Regeneration is the ability of progenitor cells to replace injured cells in a given tissue. One example of regeneration is the capability of bulge cells in the hair follicle to mend surrounding tissue (Ghysen and Dambly-Chaudiere, 2007). Located in the bulge are of the hair follicle are nestin-expressing hair follicle-associated-pluripotent (HAP) stem cells. Bulge area stem cells are able to differentiate into hair follicle matrix cells and epidermal cells (Amoh and Hoffman, 2017). Nonmammalian vertebrates, such as birds and amphibians, have exhibited the ability to partially restore hearing through the regeneration of hair cells.

Hair cell regeneration can occur via non-mitotic transdifferentiation of support cells directly into hair cells or following cellular differentiation of the resulting daughter cells (Chai et al., 2012; Kniss et al., 2016). In mice, inhibition of Notch signaling leads to hair cell differentiation within the inner ear (Ghysen and Dambly-Chaudiere, 2007). This indicates that mice possess the machinery that enables hair cell regeneration, although it has been blocked in adults. The possible ability of mice to regenerate hair cells is promising as it implies this block may be bypassed (Kniss et al., 2016). To further understand the potential for hair cell regeneration, many labs have developed techniques using the zebrafish lateral line.

In addition to the robust ability to regenerate hair cells following damage (Ma et al., 2008), the positioning of neuromasts on the surface of zebrafish is readily accessible and easy to manipulate, making it an excellent model for understanding hair cell regeneration. Following damage, such as treatment with aminoglycoside antibiotics, lateral line hair cells fully regenerate in 72 hours (Ma et al., 2008). Hair cell regeneration is dependent on the division and differentiation of support cells (Lush et al., 2019). Previous experiments using BrdU incorporation have shown that support cells in the center of neuromasts differentiate into hair cells, while peripheral support cells self-renew following proliferation (Romero-Carvajal et al., 2015).

During regeneration, a transient increase in support cell proliferation takes place 12-21 hours following damage, eventually generating new hair cells (Ma et al., 2008). There are several support cell behaviors observed during regeneration including differentiating cell divisions, support cells that divide a second time and regenerate two hair cells, amplifying cell divisions and support cell quiescence (Romero-Carvajal et al., 2015). The interplay

between the Fgf, Notch and the Wnt signaling pathway regulates self-renewal and differentiation (Romero-Carvajal et al., 2015).

The fibroblast growth factor (Fgf) signaling pathway relies on secreted signaling proteins, FGFs, to signal to receptor tyrosine kinases (FGF receptors). This pathway is found in virtually all mammalian tissues and is crucial from embryonic development to adult stages. Tissue maintenance, repair, differentiation and regeneration employ the Fgf pathway (Ornitz and Itoh, 2015). FGF and Wnt signaling pathways have been identified as key regulators in progenitor cell proliferation and regenerative cell proliferation in the zebrafish lateral line. Using a RNA in situ hybridization analysis, a 2019 study found that there was an increase in the expression of FGF pathway genes in neuromasts treated with a Wnt pathway inducer (Tang, et al., 2019). This finding proposes a strong integration of the Wnt and FGF pathways in modulating the proliferation of cells in the zebrafish neuromast.

Notch signaling factors are upregulated in neuromasts following hair cell injury and experimentally altering. Research has shown that altering Notch signaling levels results in changes in the number of regenerated hair cells, suggesting that this pathway is important for regulating hair cell number during regeneration (Thomas et al., 2015).

Pharmacological studies altering Wnt activity suggest that this pathway induces proliferation of surrounding support cells in neuromasts. This is inhibited by Notch signaling via the activation of the Wnt inhibitor Dkk2 (Thomas and Raible, 2019). The downregulation of Notch signaling is correlated to the upregulation of the Wnt target, *Wnt10a*, in central support cells (Romero-Carvajal et al., 2015). Notch signaling in the regeneration of lateral line hair cells has been well studied. The present study will focus on the involvement of the Wnt signaling pathway in the regeneration of lateral line hair cells in zebrafish.

1.4 Wnt signaling pathway

The Wnt signaling pathway is involved in crucial mechanisms during embryo development, such as cellular proliferation, migration and determination (Komiya and Habas, 2008). Previous research has suggested the involvement of the Wnt signaling pathway in regeneration of hair cells of the zebrafish lateral line regeneration, making it a pathway of interest (Romero-Carvajal et al., 2015)

Wnt is a secreted extracellular glycoprotein and acts as a ligand. Prior to transport, Wnt undergoes glycosylation in the endoplasmic reticulum. Following exocytosis, Wnt protein diffuses throughout the extracellular matrix, however this ability is limited by heparan sulfate proteoglycans (Komiya and Habas, 2008). LRP5/6 and Frizzled are Wnt receptors that turn the Wnt signaling pathway “on” when Wnt binding occurs (MacDonald and He, 2012). LRP5/6 belongs to a family of low-density lipoprotein receptor-related proteins and Frizzled is a seven transmembrane-span receptor (Huelsenken and Behrens, 2002). Mutations in LRP5 in the inner ear of zebrafish produced a decrease in cellular proliferation and reduced the number of supporting cells and hair cells, suggesting the possible importance of LRP5 in influencing the number of cells in a neuromast (Xia et al., 2017).

Intracellularly, β -catenin is the transcriptional coactivator of the canonical Wnt signaling pathway. In the absence of Wnt, cytoplasmic pools of β -catenin are targeted for degradation by a complex of proteins called the destruction complex. The destruction complex is composed of Axin, protein phosphatase 2a (PP2A), CK1, GSK-3 and β -TrCP. This complex phosphorylates β -catenin on its amino terminus, leading to ubiquitination. The ubiquitinated β -catenin is then targeted for proteasome degradation (Stamos and Weis,

2013). The destruction complex must be disrupted for β -catenin to accumulate in the cytoplasm and enter into the nucleus to act as a transcription factor.

Dishevelled (Dsh) plays an integral role in the canonical Wnt signaling pathway. Dsh is a protein that is located in the cytoplasm of cells. The protein has many functions, one of which is its ability to disrupt the destruction complex. When Wnt binds to the LRP5/6-Frizzled complex, Dsh recruits Axin and GSK3 to the receptor complex (Yamanishi et al., 2019). The recruitment of the destruction complex to the LRP5/6-Frizzled receptor complex influences the amount of β -catenin levels in the cell (Voronkov and Krauss, 2013). In addition to the ability to relocate the Axin complex, Dsh also stimulates the phosphorylation of motifs in the LRP5/6 intracellular tail that acts as a competitive inhibitor of GSK3 (Yamanishi et al., 2019). As a result of the disruption of the destruction complex, β -catenin is able to translocate to the nucleus where it acts as a transcriptional co-activator.

β -catenin is the co-activator of the T cell factors (TCF) and lymphoid enhancing factor-1 (LEF1) family of DNA binding transcription factors (Komiya and Habas, 2008). Activation of TCF/LEF results in the transcription of target genes downstream of the Wnt signaling pathway (Niida et al., 2004). In the absence of Wnt signaling, LEF1 negatively regulates the expression of Wnt signaling genes because it is bound to Groucho-related co-expressors. When β -catenin enters into the nucleus and binds to LEF1, the Groucho-related co-expressors are displaced allowing for LEF1 transcription factor activity to begin (Daniels and Weis, 2005).

Using human and mouse cell lines, researchers found that Dickkopf (Dkk1), a TCF target gene, was able to inhibit Wnt signaling. The TCF-binding elements conserved in humans and mouse are also found in the Dkk1 promoter in zebrafish (Niida et al., 2004). The

expression of Dkk1, a diffusible Wnt antagonist, is dependent upon FGF signaling (Matsuda et al., 2013). This contributes to the proposed interaction of FGF and the Wnt signaling pathway in zebrafish.

Members of the Dkk class of Wnt antagonist are secreted glycoproteins that bind to LRP5/6 and Kremen1/2 (Li et al., 2018). Dkk-1, LRP5/6 and Kremen1/2 form a ternary complex that promotes endocytosis and removal of the Wnt receptor from the plasma membrane inhibiting Wnt signaling (Mulvaney et al., 2016).

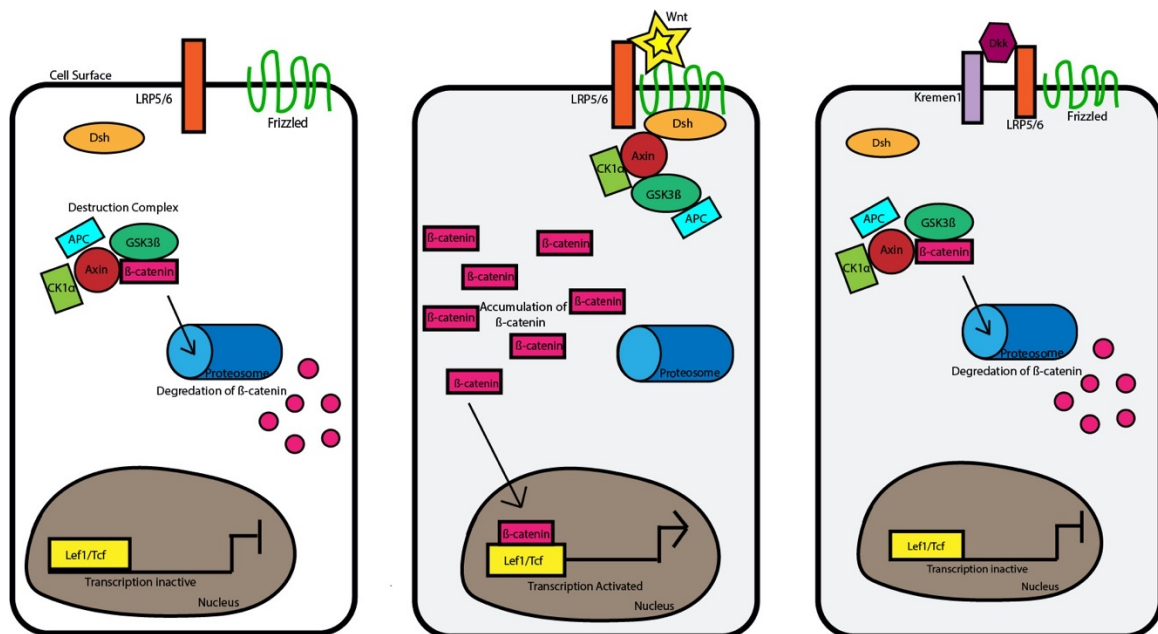


Figure 1.4. Wnt signaling pathway. Panel A details the condition of a cell when the ligand is not present. In this case, β -catenin is targeted for degradation. In panel B, Wnt is bound to Lrp5/6 and Frizzled receptors, allowing β -catenin to accumulate in the cytoplasm. In panel C, Dkk binds to Lrp5/6 and Kremen1. The complex is internalized and targeted for degradation.

1.5 Present study

Previous studies have suggested the involvement of the Wnt signaling pathway in hair cell regeneration using drugs such as 1-Azakenpaullone (AZK) (Romero-Carvajal et al., 2015). AZK is a selective GSK-3 β inhibitor (Kunick et al., 2004). The inhibition of GSK-3 β , blocks the degradation of β -catenin, this activates the Wnt signaling pathway in regenerating hair cells (Figure 1.5A).

Tankyrase is a protein that de-stabilizes Axin, which is a component of the destruction complex. When small molecule antagonists of tankyrase are present, it results in an unbalanced degradation of β -catenin (Karner et al., 2010). A study focused on the regeneration of hair cells in the avian basilar papilla used the pharmacological agent IWR-1, a tankyrase inhibitor that acts as a Wnt antagonist, to explore the involvement of the canonical Wnt signaling pathway in this process (Figure 1.5B). It was found that inhibition of the Wnt signaling pathway by IWR-1 resulted in reduced proliferation and decreased hair cell formation (Jacques et al., 2014).

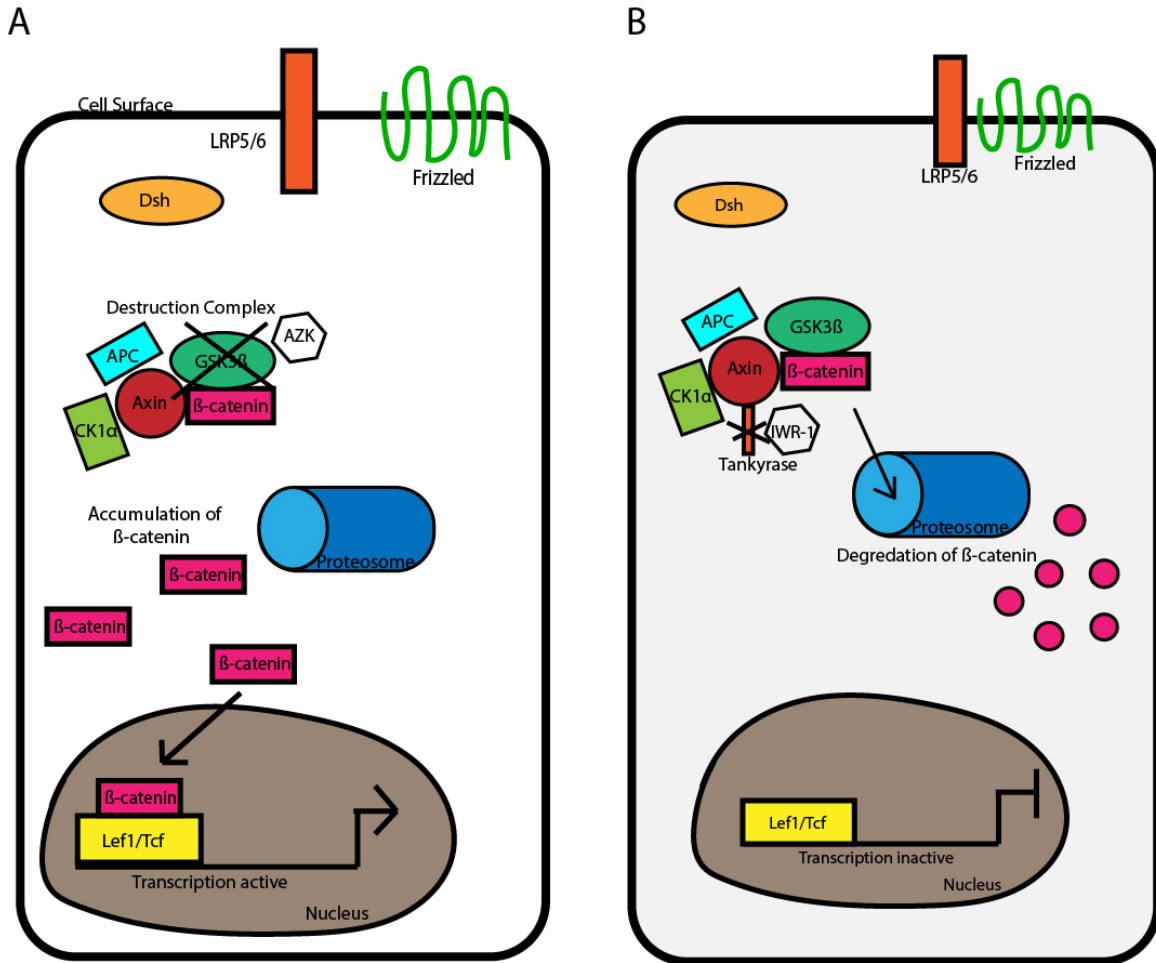


Figure 1.5. Effects of AZK and IWR-1 on the Wnt signaling pathway. Panel A shows the effect of AZK on the Wnt signaling pathway. AZK inhibits $GSK3\beta$, allowing β -catenin to accumulate. Panel B shows the effect of IWR-1 on the Wnt signaling pathway. IWR-1 blocks the effect of tankyrase, leading to an unbalanced degradation of β -catenin.

Studies employing pharmacological inhibitors and agonists of the Wnt signaling pathway strongly suggest the involvement of the canonical Wnt signaling pathway in hair cell regeneration, though these drugs have a broad range of targets, potentially complicating their specific regulation of the Wnt pathway. In this experiment, we will use Wnt pathway

mutants to more directly examine the role of Wnt signaling in regulating hair cell regeneration in the lateral line. Building on previous experiments, we used zebrafish with mutations in the *lef1*, *kremen1* and *lrp5* genes.

The mutation of the *lef1* gene disrupts the Wnt signaling pathway at the level of gene transcription. Prior experiments found that a mutation in the *lef1* gene, *lef1^{nl2}*, results in a loss of progenitor cells in the pLL primordium, resulting in defects in the establishment of proto-neuromast formation (McGraw et al., 2011). Kremen1 is a non-obligatory receptor for Dkk family proteins. When deleted, this interferes with the Wnt signaling pathway in the pLL primordium (McGraw et al., 2014). LRP5 is the co-receptor for the Wnt signaling pathway.

These three mutations disrupt Wnt signaling at different points in the pathway, with distinct consequences on cellular behaviors. It is hypothesized that the Wnt signaling pathway is crucial for lateral line mechanosensory hair cells to regenerate following damage. These mutations will disrupt the Wnt pathway, allowing us to visualize any affects this has on hair cell regeneration.

CHAPTER 2

MATERIALS AND METHODS

2.1 Staining for hair cells in the neuromast

All zebrafish used in the following protocols carried the *Tg(claudinB:lynGFP)* transgene. This transgenic line used the promotor for the *claudinB* gene to drive the membrane-localized lyn-GFP (Haas and Gilmour, 2006). Zebrafish harboring *lef1^{nl2}*, *krm1^{nl10}* or *lrp5^{nl23}* mutations and heterozygous populations, which served as the control group, were subjected to aminoglycoside antibiotic neomycin treatment at 5 days post fertilization (dpf). All dilutions were made using embryo medium, a slightly salty solution, buffered to maintain pH 7.0 (0.137 M NaCl, 5.4 mM Na₂HPO₄, 0.44 mM KH₂PO₄, 1.3 mM CaCl₂, 1.0 mM MgSO₄, 4.2 mM NaHCO₃) (Nixon et al., 2007) Neomycin sulfate was dissolved in embryo medium to yield a final concentration of 400µM. Neomycin is a member of the aminoglycoside antibiotic family and has the ability to damage hair cells (Harris et al., 2003). Fish were allowed to undergo regeneration of hair cells for 72 hours post neomycin treatment.

At 8 dpf, zebrafish were treated with FM1-43 purchased from Invitrogen ThermoFisher Scientific #F34355. FM1-43FX is a fixable styryl dye that enters into hair cells via mature mechanotransduction channels located on the apical surface of the hair cells. This attribute makes FM1-43 a key tool in marking functional hair cells (Gale et al., 2001). 15µl of FM1-43 was added to 5mL embryo medium resulting in an end concentration of 3µM. Fish were incubated with FM1-43 for 1 minute and then checked for labeling using a Zeiss Axio Zoom.V6 fluorescent dissecting microscope.

Once the FM1-43 labeling was confirmed, fish were anesthetized with tricaine in accordance to the McGraw lab UMKC IACUC protocol, and fixed using 4% paraformaldehyde/1xPBS + 4% sucrose overnight at room temperature (Thomas and Raible, 2019). The next day, fixed fish were washed with 1xPBS-0.01% Tween 20 (PBTw) for 30 minutes, three times.

Anti-parvalbumin antibody marks a family of calcium binding protein and labels all hair cells, including those that are immature and not functional (Heller et al., 2002). The monoclonal mouse P3088 Anti-Parvalbumin antibody was purchased from Sigma-Aldrich. Antibody blocking solution was made using 1x PBS, 0.01% Triton-X 100, 1% BSA, 1% DMSO and 5% goat serum. Anti-parvalbumin antibody was added to the antibody block at a ratio of 1:500. Fish were treated with the anti-parvalbumin antibody at room temperature overnight.

The following day, fish were washed with PBTw three times for 30 minutes each. Alexa 647 is a goat anti-mouse IgG (H+L) cross-absorbed secondary antibody, A-21235, purchased from Invitrogen ThermoFisher Scientific. This secondary antibody was added to the block in a ratio of 1:1000. Fish were incubated in antibody block overnight at room temperature. Three PBTw washes were performed for a period of 20 minutes each, followed by a 1xPBS wash. Fish were treated for 15 minutes with 10mM Diamidino-2-phenylindole (DAPI), a stain that marks chromosomes in the nuclei of every cell of the larvae (Estandarte et al., 2016) purchased from ThermoFisher Scientific. Once DAPI staining was confirmed using a Zeiss Axio Imager.D2 fluorescent microscope, fish were stored in 50% glycerol + 50% 1xPBS.

Table 2.1

<i>Days post fertilization</i>	<i>Treatment Performed</i>
3 dpf	Sorted larvae by mutation
5 dpf	Induced hair cell death with neomycin
8 dpf	FM1-43 labeling
	Fixation with 4% PFA
	Anti-Parvalbumin staining

FM1-43 and anti-parvalbumin staining protocol.

2.2 Identifying cellular proliferation in neuromasts

The synthetic nucleoside, Bromodeoxyuridine (BrdU), is an analog of thymidine (Cavanagh et al., 2009) purchased from Invitrogen ThermoFisher Scientific. BrdU is incorporated into synthesizing DNA during S-phase in dividing cells, making it a prime indicator of proliferation (Harris et al., 2003). To perform BrdU staining, homozygous and heterozygous fish populations were divided in a 6-well plate. Larvae were treated with 400 μ M neomycin as describe above, prior to incubation in BrdU.

The neomycin treated fish were transferred to new wells containing 10mM BrdU and 1% DMSO in embryo medium and incubated at 28°C for 24 hours. Fish were then

transferred to fresh embryo medium and incubated for an additional day at 28°C. Fish were anesthetized with tricaine and transferred into 1.5mL collection tubes. 4% paraformaldehyde/1xPBS was used for fixation, which took place for 2 hours at room temperature. Three 20-minute washes were performed using PBS-D-T (49.5mL 1xPBS, 500µL DMSO and 50µL of tween-20) (Harris et al., 2003). Next, PBDT washes took place three times for 20 minutes each. Fish were transferred to methanol before being incubated overnight at -20°C. After incubation, fish were washed in a stepwise fashion, beginning with 75% MeOH (w/1xPBS), followed by 50% MeOH (w/1xPBS) and then 25% MeOH (w/1xPBS), each for 20 minutes.

Once a 20-minute wash of PBDT took place, a digestion was performed using proteinase K (10µg/mL) in PBDT for 10 minutes. Next, fish were refixed using 4% PFA for 20 minutes. 5-minute washes with PBDT were performed three times, before incubating for 1 hour at room temperature in 1N HCl. Three PBDT washes were performed for five minutes each. A block solution, 10% normal goat serum in PBDT, was made up using 900µL PBDT and 100µL of goat serum. Fish were incubated for a minimum of 1 hour in the block solution at room temperature.

Monoclonal mouse anti-BrdU antibody, B2531, was purchased from Sigma-Aldrich. Anti-BrdU antibody was added to the block at a ratio of 1:400. Fish were treated with the primary antibody overnight, before undergoing three 20-minute washes using PBDT. The secondary antibody, Alexa 586 goat anti-mouse IgG (H+L) cross-absorbed secondary antibody, A-11004, was purchased from Invitrogen ThermoFisher Scientific and was added to the block at a ratio of 1:400. Incubation with the secondary antibody occurred for a minimum of 5 hours at room temperature. Three 20-minute washes with PBTw took place,

followed by a quick 1xPBS wash. Lastly, the nuclei were stained using DAPI before being stored in 50% glycerol/1xPBS at 4°C.

Table 2.2

<i>Days post fertilization</i>	<i>Treatment Performed</i>
3 dpf	Sorted larvae by mutation
5 dpf	Induced hair cell death with neomycin
5-6 dpf	BrdU treatment
7 dpf	Fixation with 4% PFA Anti-body labeling and DAPI staining

BrdU and DAPI staining protocol

2.3 Treatment with AZK

1-Azakenpaullone (AZK) is a pharmacological drug that disrupts the destruction complex, halting the degradation of β -catenin. Previous research used 3 μ M of the drug, however we were not able to replicate these results during hair regeneration, though other phenotypes suggesting increased Wnt activity were detected in larvae (data not shown)

(Romero-Carvajal et al., 2015). We increased the drug concentration to 15 μ M for this experiment.

At 5dpf, fish were immersed in 15 μ M of AZK dissolved in dimethylsulfoxide (DMSO). As a control, a group of fish were exposed to an equal volume of DMSO only. After being exposed to the drug for 1 hour at room temperature, fish were treated with neomycin for 30 minutes at 28°C as described above. Fish were then rinsed and transferred to wells containing either AZK or DMSO. A 3-day incubation was allowed for regeneration.

At 8dpf, fish were removed from embryo medium and anesthetized using tricaine, followed by fixation using paraformaldehyde. FM1-43, anti-parvalbumin and BrdU experiments were then performed following previously described protocols.

Table 2.3

Days post fertilization Treatment Performed

<i>5 dpf</i>	AZK or DMSO treatment Induced hair cell death with neomycin
<i>5-6 dpf</i>	Incubated in embryo medium
<i>8 dpf</i>	FM1-43/anti-parv treatment or BrdU/DAPI treatment

AZK and DMSO treatment protocol

2.4 Treatment with IWR

IWR-1 is a drug that has been shown to inhibit the canonical Wnt signaling pathway (Sigma-Aldrich I0161). To replicate the effect of IWR-1 on regeneration (Jacques et al., 2014), we treated a group of zebrafish to this pharmacological agent. Two groups of zebrafish were used for this experiment. The first group was treated with 22 μ M of IWR-1 and the second group served as a control using an equal volume of DMSO.

The two groups were isolated from each other using a 6-well plate. The zebrafish were incubated with IWR-1 or DMSO for 1 hour at 28°C. Next, they were exposed to neomycin for 30 minutes at 28°C to kill off existing hair cells. Following neomycin treatment, fish were used for either FM1-43/Anti-parvalbumin or BrdU experiments as previously described.

Table 2.4

<i>Days post fertilization</i>	<i>Treatment Performed</i>
5 dpf	IWR-1 or DMSO treatment Induced hair cell death with neomycin
5-6 dpf	Incubated in embryo medium
8 dpf	FM1-43/anti-parv treatment or BrdU/DAPI treatment

IWR-1 and DMSO treatment protocol

2.5 Data Collection and analysis

Images of neuromasts were taken using the 20x objective lens on a Zeiss Axio Imager.D2 fluorescent compound upright microscope. The 647nm channel was used to image anti-parvalbumin, the 405nm channel for DAPI, the 488nm channel for GFP and the 568nm channel for FM1-43 or BrdU. Each image taken contained one to three neuromasts. All cells in the neuromasts were visualized using DAPI staining. The number of cells in a given neuromast were counted and recorded. Counting was also performed based on the number of cells marked with anti-parvalbumin antibody, FM1-43 and BrdU.

When heterozygous zebrafish carrying a given mutation lay eggs, a quarter will be homozygous and the rest will be heterozygous or wildtype. Larvae from *lrp5^{nl23}*, *lef1^{nl2}* and *krm1^{nl10}* mutant lines were kept separate. Each group contained both homozygous and heterozygous progeny. Homozygous mutants were compared to their heterozygous siblings, which served as the control. After completing the cell count, the homozygous and corresponding heterozygous populations were compared to each other. The data analysis program, GraphPad Prism version 8.4.3, was used to perform an unpaired Student's T-test and to generate data charts.

2.6 Imaging neuromasts using confocal microscopy

lrp5^{nl23}, *lef1^{nl2}* and *krm1^{nl10}* mutants and heterozygous sibling, IWR-1, AZK and DMSO treated neuromasts were imaged using the 40x oil objective lens of a Zeiss 510 fluorescent confocal microscope. Once the images were obtained, they were processed using Fiji-Image J and the brightness and contrast were adjusted using Adobe PhotoShop to create uniformity between images (Schindelin et al., 2012).

CHAPTER 3

RESULTS

3.1 Introduction to results

It is hypothesized that the Wnt signaling pathway is critical for both neuromast development in the zebrafish lateral line and hair cell regeneration following damage. Three mutant fish lines were used to test this hypothesis: the first is a null mutation in the Lef1 transcription factor; second, a null mutation in the non-obligatory co-receptor, Kremen1, which acts with the ligand Dkk1 to inhibit the Wnt signaling pathway; and finally, a null mutation of the Wnt co-receptor, LRP5, were examined.

3.2 Eight-day regeneration in *lef1^{nl2}* mutants

Lef1 is a transcription factor for the Wnt signaling pathway that is activated when β -catenin binds to it (Daniels and Weis, 2005). Once Lef1 is activated, it proceeds to activate transcription of downstream target genes of the Wnt signaling pathway (Doupas et al., 2019).

When the Lef1 transcription factor function is inhibited, transcription of downstream Wnt target genes is halted (Daniels and Weis, 2005) (figure 3.2A). The *lef1^{nl2}* mutation downregulates the effects of Wnt signaling and results in fewer hair cells produced during regeneration. In addition, the following results show that proliferation is unaffected in zebrafish harboring a homozygous mutation in the *lef1^{nl2}* transcription factor. This suggests that Lef1 is obligatory for specification of hair cells during regeneration but has no effect on cellular proliferation in the zebrafish lateral line.

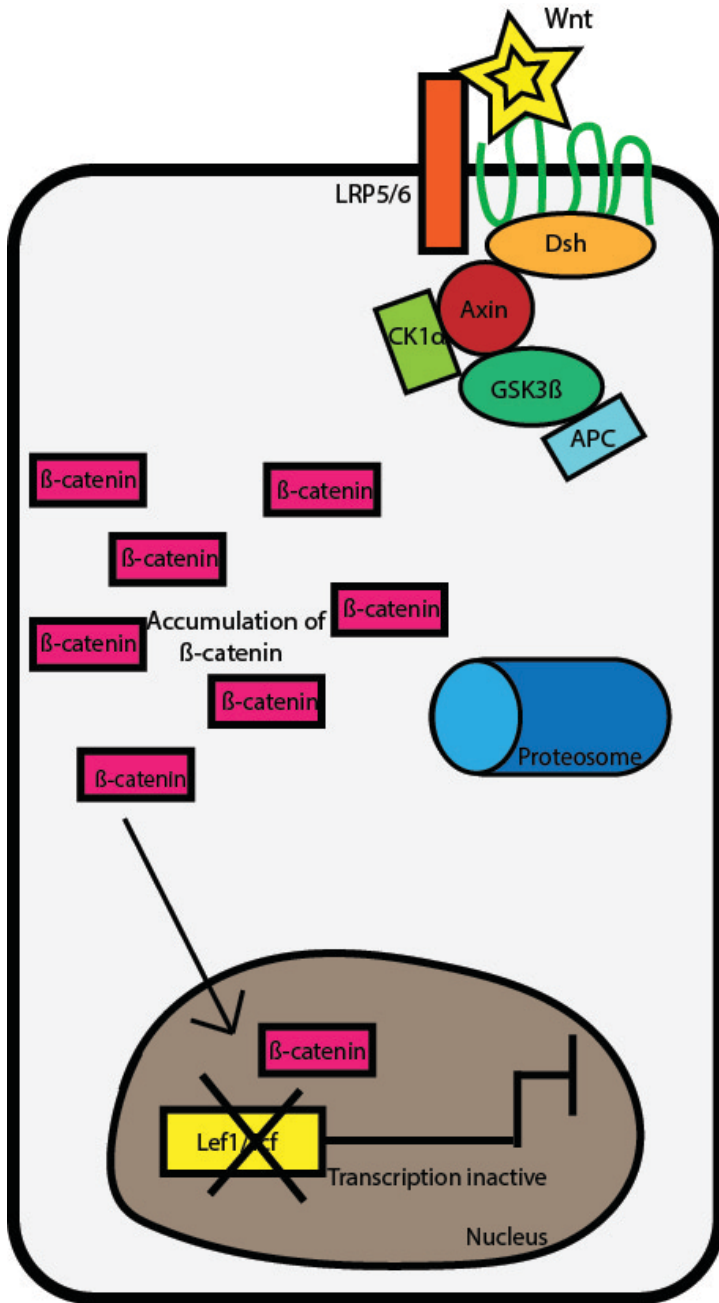


Figure 3.2A. When the Lef1 transcription factor is not present, transcription of downstream target genes is not possible.

Previous studies have demonstrated that *Lef1* is required for posterior lateral line formation (McGraw et al., 2001; Valdavia et al., 2011). It is hypothesized that a mutation in the *Lef1* transcription factor disrupts the Wnt signaling pathway affecting regeneration of hair cells in the zebrafish lateral line.

Zebrafish larvae with the *lef1^{nl2}* mutation and heterozygous zebrafish larvae were compared based on the number of functional hair cells observed in the lateral line neuromasts following regeneration. 20 heterozygous larvae had an average of 5.819 functional hair cells per neuromast. Images of FM1-43+ cells in a neuromast of the heterozygous larva can be seen in figure 3.2 A''. The *lef1^{nl2}* homozygous population composed of 25 larvae that were treated with FM1-43 labelling. Functional hair cells were counted in each neuromast and the calculated average was 4.453. A visual reference of FM1-43+ cells can be seen in figure 3.2 B''. The *lef1^{nl2}* mutant and heterozygous sibling populations were compared to one another via an unpaired Student's T-test. The p-value was calculated to be <0.0001, demonstrating a statistical difference. A graph comparing the averages of each population can be seen in figure 3.2 C.

The anti-parvalbumin antibody was utilized to label each hair cell in a given neuromast, without regard to functionality. 24 zebrafish larvae homozygous for the *lef1^{nl2}* mutation were compared to a population of 20 zebrafish larvae heterozygous for the *lef1^{nl2}* mutation. The heterozygous population provided a positive control for this experiment. An average of 6.532 hair cells were counted in the heterozygous population (Figure 3.2 A'''). The homozygous group had an average of 5.023 hair cells in a given neuromast (Figure 3.2 B'''). When compared using an unpaired Student's T-test, the populations were found to be statistically different with a p-value of <0.0001 (Figure 3.2D). The statistical differences observed in the

FM1-43 and anti-parvalbumin stained zebrafish infers that the *lef1^{n/2}* mutation disrupts the Wnt signaling pathway, resulting in defects in regeneration of hair cells in later development of larvae.

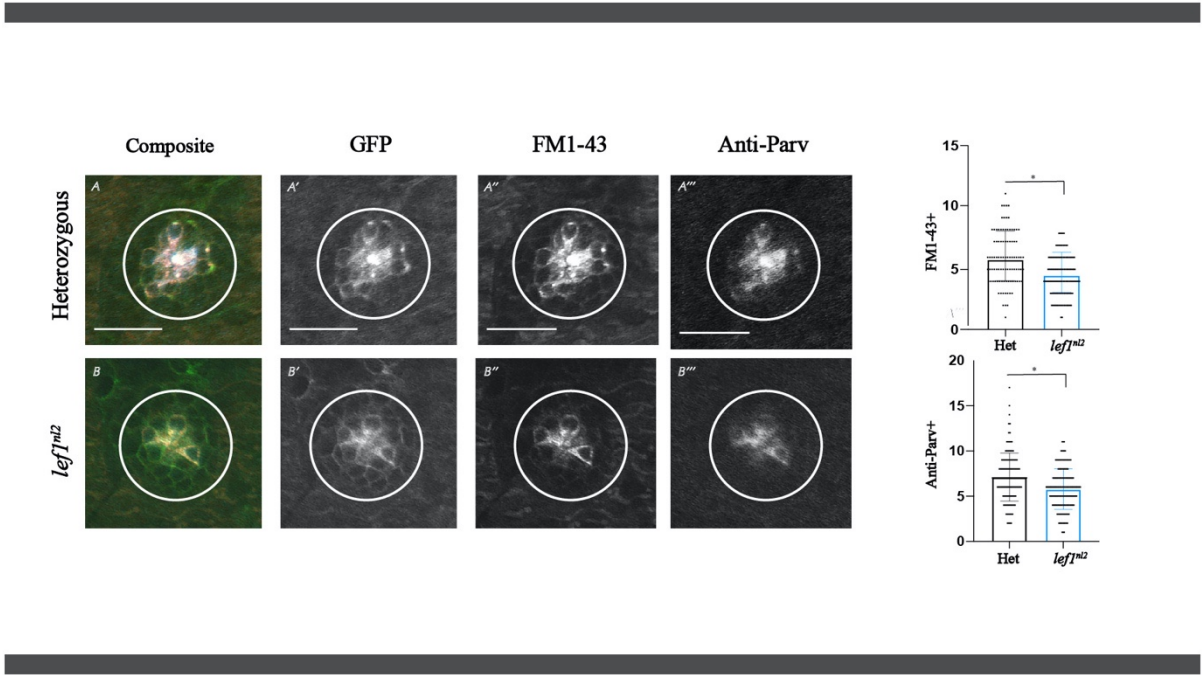


Figure 3.2. Confocal images were taken of *lef1^{n/2}* homozygous and heterozygous neuromast following hair cell regeneration. White circles denote the location of neuromasts in each confocal image. The heterozygous neuromast is shown in panels A-A'''. Homozygous neuromasts are shown in panels B-B'''. The scale bar equals 20nm. Panels A and B show composites including all staining conditions. Panels A' and B' are images of GFP. Panels A'' and B'' distinguish FM1-43+ cells. Panels A''' and B''' imaged anti-parvalbumin+ cells. Panel C represents the difference in FM1-43+ cells between heterozygous and homozygous neuromasts. Panel D represents the difference in FM1-43+ cells between heterozygous and homozygous neuromasts. The p-value was <0.0001. The scale bar represents 20µm.

3.3 Cell proliferation in *lef1^{nl2}* homozygous neuromasts

We next used BrdU incorporation into replicating DNA to assess proliferation during regeneration. 11 zebrafish *lef1^{nl2}* heterozygous larvae were compared to a population of 12 zebrafish larvae carrying a homozygous mutation of the Lef1 transcription factor. An average number of BrdU+ cells in the heterozygous group was counted to be 12.37 cells. For the *lef1^{nl2}* homozygous fish, the average number of BrdU+ cells were 10.65. When the two population were compared using an unpaired Student's T-test, the p-value was calculated to be 0.0959 and therefore not significant (Figure 3.3 C).

DAPI binds to adenine and thymidine rich clusters in the minor groove of double stranded DNA, marking every cell in the larvae (Chazotte, 2011) (Figure 3.3 A and B). 11 zebrafish heterozygous for the *lef1^{nl2}* mutation were compared to 12 *lef1^{nl2}* homozygous fish. For the heterozygous population, there was an average of 32.63 cells per neuromast. The *lef1^{nl2}* homozygous fish had an average of 28.26 DAPI+ cells per neuromast (Figure 3.3 D). When compared, the calculated p-value was 0.0207, indicating a small decrease in the average total number of cells in the neuromasts of *lef1^{nl2}* mutants following regeneration.

P-values from the FM1-43 and anti-parvalbumin experiments indicate that there is a statistically significant difference in regeneration of homozygous and heterozygous fish larvae. Although, there was no statistical difference between proliferating cells in the neuromast. This is of interest because it suggests that the *lef1^{nl2}* mutation does not disrupt proliferation, but rather hair cell differentiation during regeneration.

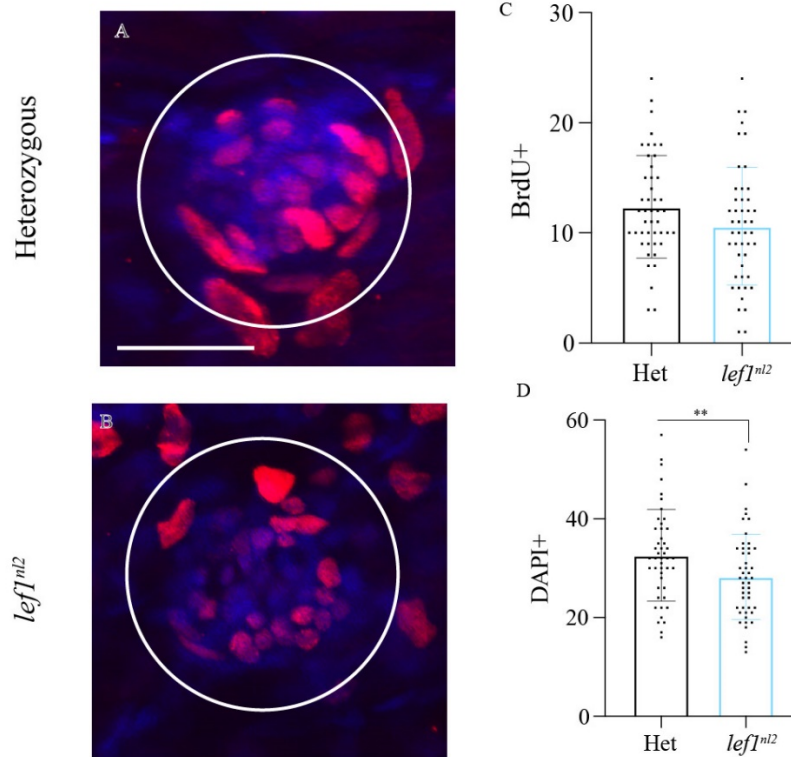


Figure 3.3. Cellular proliferation in *lef1ⁿ¹²* homozygous and heterozygous siblings following regeneration. The white circles encompass the neuromasts of heterozygous and *lef1ⁿ¹²* homozygous neuromasts. Panel A is an image of a heterozygous neuromast taken with a confocal microscope. Panel B is an image of a *lef1ⁿ¹²* homozygous neuromast taken with a confocal microscope. DAPI+ cells are shown in blue and BrdU+ cells are shown in red. Panel C represents the BrdU+ cell averages between heterozygous and homozygous fish. The p-value was calculated to be 0.0959. Panel D represents the average DAPI+ cells counted in heterozygous and homozygous neuromasts. The p-value was calculated to be 0.0207. The scale bar represents 20 μ m.

3.4 Eight-day regeneration in *krm1ⁿ¹¹⁰* mutants

Kremen1 is a non-obligatory receptor for the ligand Dkk. When Dkk binds to Kremen1 and LRP5, it causes an internalization of the receptor complex (Mulvaney et al.,

2016). Internalization of LRP5 makes it impossible for Wnt to bind, therefore downregulating the Wnt signaling pathway (Mulvaney et al., 2016). The following results demonstrate that in that a null mutation in Kremen1 decreases Dkk inhibition, allowing upregulation of Wnt activity, resulting in an increase in the overall number of hair cells and the number of functioning hair cells in a neuromast (Figure 3.1 B).

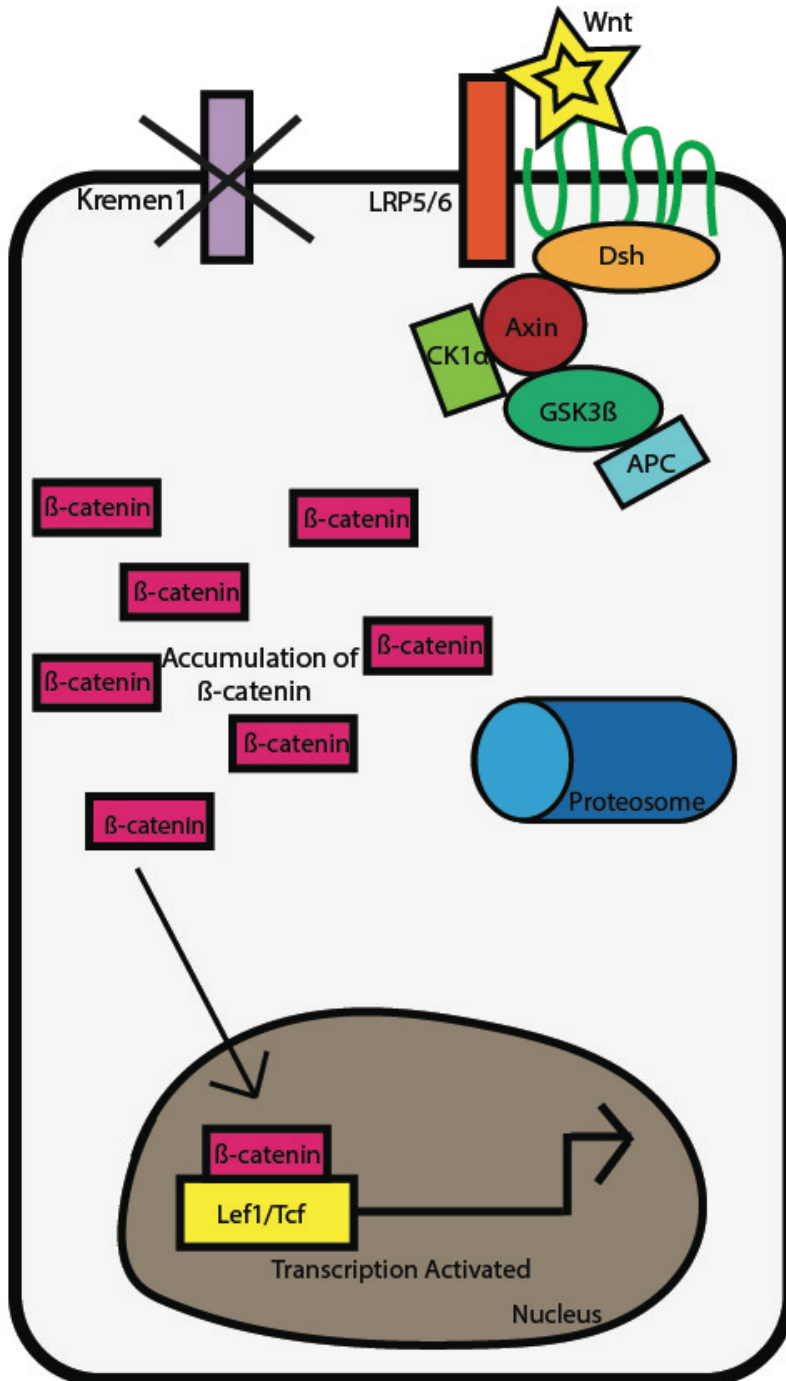


Figure 3.4A. Null mutation of the Kremen1 co-receptor. A null mutation in the Kremen1 receptor prevents Dkk inhibition, allowing for the accumulation of β -catenin.

FM1-43 staining was used to label all functional hair cells in the *krm1^{nl10}* mutant group and its corresponding heterozygous control group. There were 23 heterozygous fish treated with FM1-43 dye. The average number of functional hair cells for this group was 5.475 per neuromast (figure 3.4 A''). 13 *krm1^{nl10}* homozygous mutants had an average of 7.032 functional hair cells per neuromast (Figure 3.4 B''). When compared together, the number of hair cells counted for each group were statistically different. A Student's T-test calculated a p-value of <0.0001 and the *krm1^{nl10}* mutants were shown to have a greater amount of functional hair cells (Figure 3.4 C).

Anti-Parvalbumin antibody was used to visualize every hair cell in the neuromasts, including hair cells that are not actively functioning. The *krm1^{nl10}* heterozygous control group consisted for 23 zebrafish larvae. The number of anti-parvalbumin+ cells in the heterozygous neuromasts averaged 5.861 hair cells (Figure 3.4 A'''). 13 zebrafish *krm1^{nl10}* mutant larvae were subjected to anti-parvalbumin antibody staining. The number of hair cells in each neuromast was counted and the average amount per neuromast was 7.556 (figure 3.4 B''').

Anti-parvalbumin data for each condition was analyzed using an unpaired Student's T-test, which showed a significant difference (p: <0.0001). Please refer to figure 3.4 D. for a graph detailing the difference in *krm1^{nl10}* homozygous and heterozygous anti-parvalbumin stained cells. Kremen1 is a co-receptor for Dkk inhibition of Wnt signaling (Mulvaney et al., 2016). The data presented suggests that in the absence of Kremen1, the Wnt signaling pathway is upregulated. Therefore, supporting the notion that the Wnt pathway is involved in hair cell regeneration.

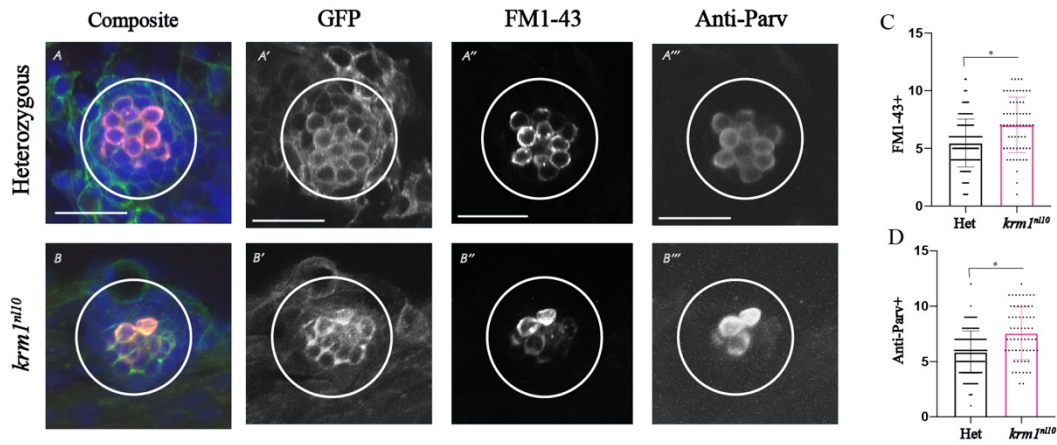


Figure 3.4. Confocal images of *krm1^{nl10}* homozygous and heterozygous neuromasts following regeneration. Panels A-A''' are confocal images taken of a heterozygous neuromast at 8dpf and 3 days post neomycin treatment. Panels B-B''' are confocal images of *krm1^{nl10}* homozygous neuromasts. The white circles encapsulate each neuromast. Panel C represents the calculated FM1-43+ average for each condition. Panel D represents the calculated Anti-parvalbumin+ average. The p-value was <0.0001. The scale bar represents 20 μ m.

3.5 Cell proliferation in *krm1^{nl10}* mutant neuromasts

In these experiments, 19 zebrafish *krm1^{nl10}* heterozygous larvae and 13 zebrafish *krm1^{nl10}* homozygous fish larvae were subjected to BrdU staining to visualize cellular proliferation in the neuromasts. The *krm1^{nl10}* heterozygous neuromasts had an average of 12.99 BrdU+ (image 3.5 A). The *krm1^{nl10}* mutant zebrafish had an average of 11.98 BrdU+ cells per neuromast (Figure 3.5 B). An unpaired Student's T-test was performed to compare the *krm1^{nl10}* homozygous and heterozygous groups. A p-value of 0.261 was calculated,

revealing the two populations to have no statistical difference in neuromast cell proliferation (Figure 3.5 C).

The *krm1^{nl10}* heterozygous group consisted of 19 zebrafish larvae and the homozygous group contained 13 zebrafish larvae. Following treatment with BrdU+, fish were fixed and stained with DAPI. The average wildtype neuromast was comprised of 31.57 DAPI+ cells. An average of 33.62 cells were counted in the homozygous *krm1^{nl10}* mutant neuromast. The two groups showed no statistical difference when analyzed using an unpaired Student T-test ($p=0.1196$). FM1-43 and anti-parvalbumin labelling demonstrated that an increase in functioning and overall hair cell count was observed in the *krm1^{nl10}* mutant. However, there was no statistical difference in proliferation or the number of cells in a neuromast (Figure 3.5 D). This suggests that the Wnt signaling pathway plays a role in hair cell specification rather than proliferation.

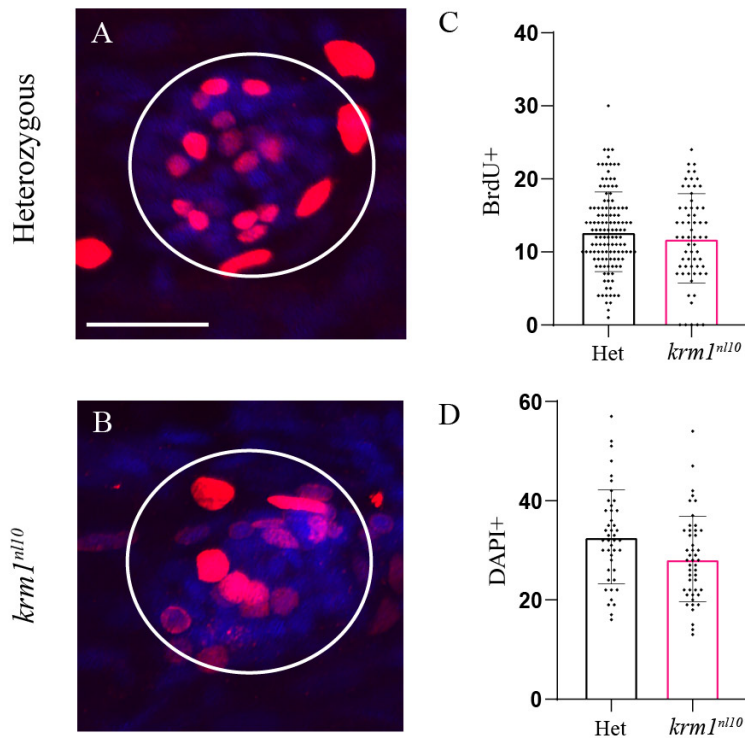


Figure 3.5. Cellular proliferation in a *krm1^{nl10}* homozygous and heterozygous neuromast. Panel A is a confocal image of a heterozygous neuromast treated with BrdU and DAPI staining. BrdU+ cells are represented in red and DAPI+ cells appear in blue. The white circle surrounds the neuromast in each image. Panel C shows the averages for BrdU+ cells in heterozygous and *krm1^{nl10}* homozygous neuromasts. The p-value was 0.261. Panel D shows the averages for DAPI+ cells in heterozygous and homozygous neuromasts. The p-value was 0.1196. The scale bar represents 20µm.

3.6 Eight day regeneration in *lrp5^{nl23}* mutants

LRP5 is a co-receptor for the Wnt signaling pathway. When Wnt binds to LRP5 and Frizzled the destruction complex is disrupted, allowing for the accumulation of β -catenin. A

null mutation of LRP5 prevents Wnt binding, resulting in the degradation of β -catenin (Figure 3.1 C).

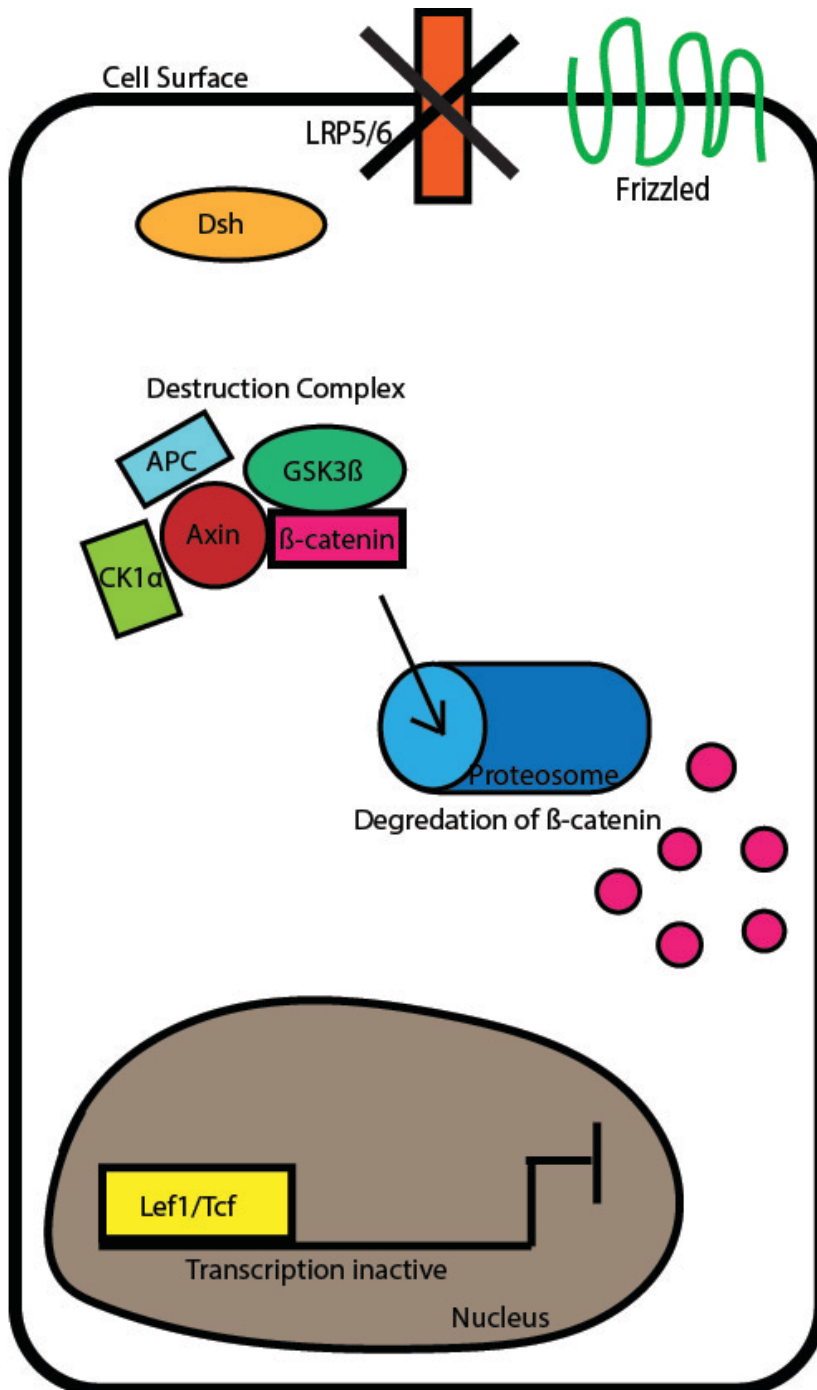


Figure 3.6A. *lrp5^{nl23}* null mutation. The null mutation of Lrp5 prevents the binding of the Wnt ligand, therefore allowing the destruction complex to target β -catenin for degradation.

lrp5^{nl23} homozygous and heterozygous fish were subjected to treatment with FM1-43 to label all functioning hair cells in each neuromast. 18 zebrafish heterozygous for the *lrp5^{nl23}* mutation had an average of 6.238 functioning hair cells in a given neuromast (figure 3.6 A''). An average of 6.103 FM1-43+ cells in *lrp5^{nl23}* homozygous fish were counted using ImageJ and Photoshop (figure 3.6 B''). An unpaired Student's T-test computed a p-value of 0.1543 when comparing the two population. This p-value states that there was no significant difference between heterozygous and homozygous zebrafish larvae (figure 3.6 C).

Anti-parvalbumin was used to mark every hair cell present in a neuromast. The average number of anti-parvalbumin+ cells in a group of 18 *lrp5^{nl23}* heterozygous zebrafish larvae was 6.848 (Figure 6 A'''). The *lrp5^{nl23}* homozygous population was made up of 14 zebrafish larvae. The average anti-parvalbumin+ cells the neuromasts of *lrp5^{nl23}* homozygous zebrafish was 6.897 (figure 6 B'''). An unpaired Student's T-test determined that there was no significant difference between the number of anti-parvalbumin+ cells in each group (p=0.1418) (Figure 3.6D). The lack of statistical difference between the average functioning hair cells and the total number of hair cells suggest that the loss of LRP5 is not sufficient to disrupt Wnt signaling in the zebrafish lateral line.

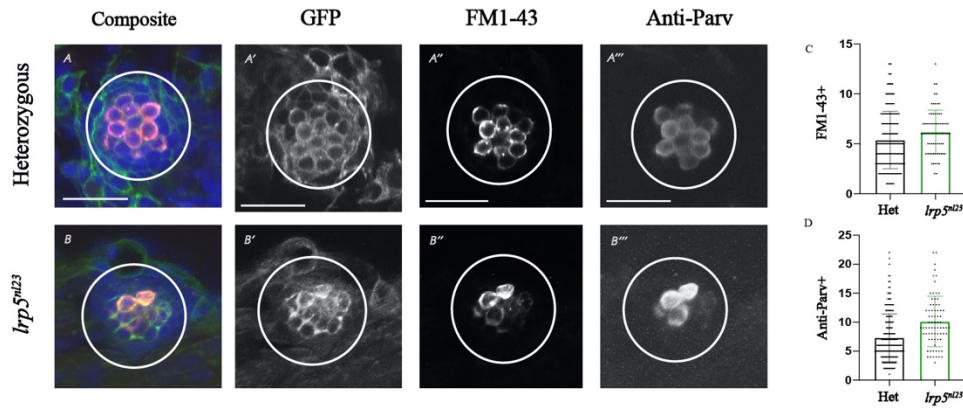


Figure 3.6. Confocal images were taken of a *lrp5^{nl23}* homozygous and heterozygous neuromast following regeneration. Panels A-A''' are images taken of a heterozygous neuromast by a confocal microscope. Panels B-B''' are images taken of a *lrp5^{nl23}* homozygous neuromast by a confocal microscope. The white circles highlight each neuromast. Panel C is representative of the calculated FM1-43+ averages of heterozygous and *lrp5^{nl23}* homozygous neuromasts. The p-value is 0.1543. Panel D is representative of the calculated anti-parvalbumin+ averages of heterozygous and *lrp5^{nl23}* homozygous neuromasts. The p-value is 0.1543. The scale bar represents 20 μm.

3.7 Cell proliferation in *lrp5^{nl23}* mutant neuromasts

Cellular proliferation in *lrp5^{nl23}* heterozygous and *lrp5^{nl23}* homozygous fish was determined by counting the number of BrdU+ cells in each neuromast using ImageJ and Photoshop. 20 zebrafish larvae made up the *lrp5^{nl23}* heterozygous population and the LRP5 homozygous population comprised of 17 zebrafish. The average BrdU+ cells in a given heterozygous neuromast was 12.13 (Figure 3.7 A). The average of BrdU+ in the *lrp5^{nl23}* homozygous population was 8.456 BrdU+ cells in the neuromasts (Figure 3.7 A). An

unpaired Student's T-test revealed a significant difference with the p-value equaling <0.0001 (Figure 3.7 C).

To identify every cell in a neuromast, DAPI staining was used. The *lrp5^{nl23}* heterozygous fish group consisted of 20 zebrafish larvae. The average number of DAPI+ cells in a neuromast was 29.06. 17 zebrafish larvae were included in the *lrp5^{nl23}* homozygous group. The average number of DAPI+ cells in the neuromasts was 25.6. An unpaired Student's T-test calculated a p-value of 0.0048, which demonstrated a statistical difference (Figure 3.7 D). When compared to the analysis of FM1-43 and anti-parvalbumin, which did not show a statistical difference, it can be concluded that LRP5 is not critical for specification, but rather is necessary for proliferation and cell numbers in the zebrafish neuromasts.

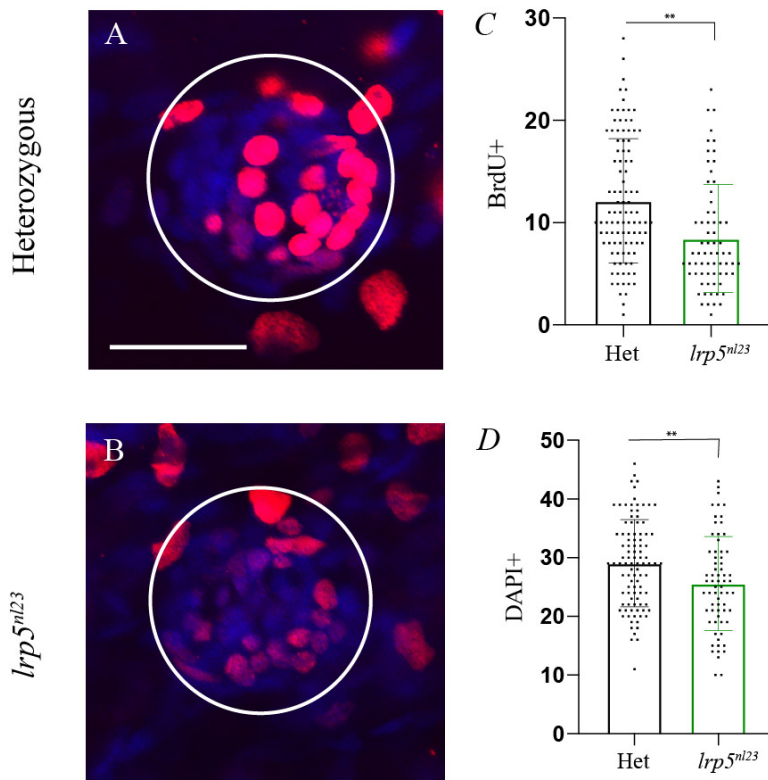


Figure 3.7. Cellular proliferation in a *lrp5^{nl23}* homozygous and heterozygous neuromast. Panel A is a confocal image taken of a heterozygous neuromast and panel B is a confocal image of a *lrp5^{nl23}* homozygous neuromast. BrdU+ cells are shown in red. DAPI+ cells are shown in blue. Panel C represents the calculated averages of heterozygous and *lrp5^{nl23}* homozygous BrdU+ cells in a neuromast. The p-value is <0.0001. Panel D represents the calculated averages of heterozygous and *lrp5^{nl23}* homozygous DAPI+ cells in a neuromast. The p-value is 0.0048. The scale bar represents 20 μ m.

3.8 Eight day regeneration of AZK treated fish

Zebrafish larvae containing no mutations were subjected to an AZK drug treatment.

AZK is a pharmacological agent that upregulates the Wnt signaling pathway (Jacques et al.,

2014). Research has been performed using 3 μ M of AZK dissolved in DMSO. However, these results were not replicable in our hands. In this experiment, we increased the drug concentration to 15 μ M to investigate potential effects on regeneration. After drug treatment, fish were treated with FM1-43 and stained with anti-parvalbumin antibody.

Fish were either treated with 15 μ M of AZK dissolved in DMSO or with DMSO alone. The DMSO treated group consisted of 17 larvae and the AZK treated group consisted of 20 larvae. The average number of FM1-43+ cells in the control group was 4.979. In the AZK treated fish, the average was 5.103 FM1-43+ cells. There was no significant difference when the two groups were compared using an unpaired Student's T-test ($p=0.5842$).

Anti-parvalbumin was used to mark all hair cells in the neuromast, regardless of functionality. The DMSO group had an average of 6.086 anti-parvalbumin+ cells. An average of 6.224 anti-parvalbumin+ cells was observed in AZK treated fish. The two groups were compared using an unpaired Student's T-test and no statistical difference was found ($p=0.5888$).

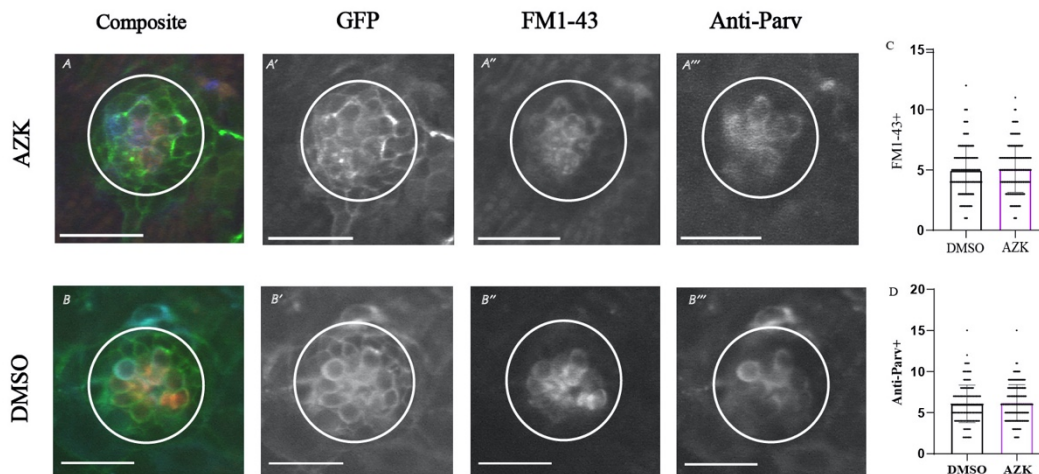


Figure 3.8. Confocal images of AZK and DMSO treated fish following regeneration. Panels A-A''' are images taken of an AZK treated neuromast by a confocal microscope. Panels B-B''' are images taken of a DMSO treated neuromast by a confocal microscope. The white circles highlight each neuromast. Panel C is representative of the calculated FM1-43+ averages of AZK and DMSO treated neuromasts. The p-value is 0.5842. Panel D is representative of the calculated anti-parvalbumin+ averages of DMSO and AZK treated neuromasts. The p-value is 0.5888. The scale bar represents 20µm.

3.9 Cell proliferation in AZK treated neuromasts

To examine proliferation, 14 DMSO treated zebrafish were exposed to BrdU in this experiment. The average number of BrdU+ cells in this condition was 12.66. The AZK treated group consisted of 14 zebrafish larvae. The average number of BrdU+ cells in this group was 13.48. A p-value of 0.2522 was obtained from an unpaired Student's T-test. This value denotes no statistical difference between the two conditions. We used DAPI labeling to examine total cell numbers and found that the average number of DAPI+ cells in DMSO

treated fish was 28.27. An average of 30.19 DAPI+ cells was calculated for the AZK treated group. When compared statistically with an unpaired Student's T-test, the p-value was found to be 0.1241. This p-value demonstrated that there was no significant difference in the total number of cells in the DMSO and AZK treated neuromasts.

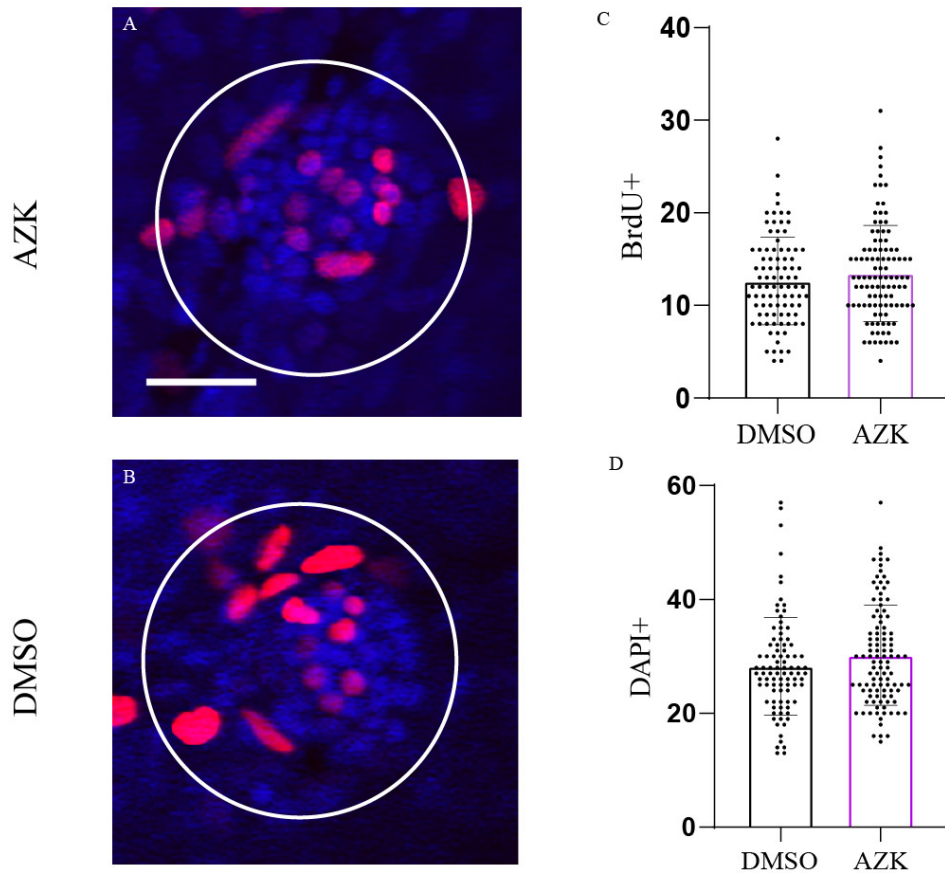


Figure 3.9. Cellular proliferation in an AZK and DMSO treated neuromast. Panel A is a confocal image taken of an AZK treated neuromast and panel B is a confocal image of a DMSO treated neuromast. BrdU+ cells are shown in red. DAPI+ cells are shown in blue. Panel C represents the calculated averages of DMSO and AZK BrdU+ cells in a neuromast. The p-value is 0.2522. Panel D represents the calculated averages of DMSO and AZK DAPI+ cells in a neuromast. The p-value is 0.1241. The scale bar represents 20 μ m.

3.10 Eight day regeneration of IWR treated fish

Zebrafish larvae were either treated with IWR-1 or DMSO. It was previously shown that IWR-1 is an inhibitor of the Wnt signaling pathway. Both conditions were subjected FM1-43

staining while still viable. Once fixed, the zebrafish underwent anti-parvalbumin staining. FM1-43 is taken up by active mechanotransduction channels in hair cells, therefore only marking functioning hair cells. Anti-parvalbumin marks all hair cells regardless of functionality.

The IWR-1 group treated with FM1-43 and anti-parvalbumin consisted of 20 zebrafish. The average number of FM1-43+ cells in the IWR-1 treated group was 3.489. The DMSO treated group consisted of 10 zebrafish and had an average of 5.06 FM1-43+ cells. When compared using an unpaired Student's T-test, a calculated p-value of <0.0001 was obtained (Figure 3.10).

20 IWR-1 treated zebrafish were stained with anti-parvalbumin. The average number of anti-parvalbumin+ cells in the IWR-1 treated group was 4.191. The DMSO treated group was made up of 10 zebrafish and had an average of 5.702 anti-parvalbumin+ cells. When compared using an unpaired Student's T-test, a p-value of <0.0001 was calculated (3.10). The obtained results of the FM1-43 and anti-parvalbumin experiments using IWR-1 as an inhibitor of the Wnt signaling pathway, suggests the involvement of the canonical Wnt signaling pathway in hair cell regeneration. This statement is supported by the results obtained that demonstrated a greatly reduced number of lateral line hair cells in IWR-1 treated zebrafish.

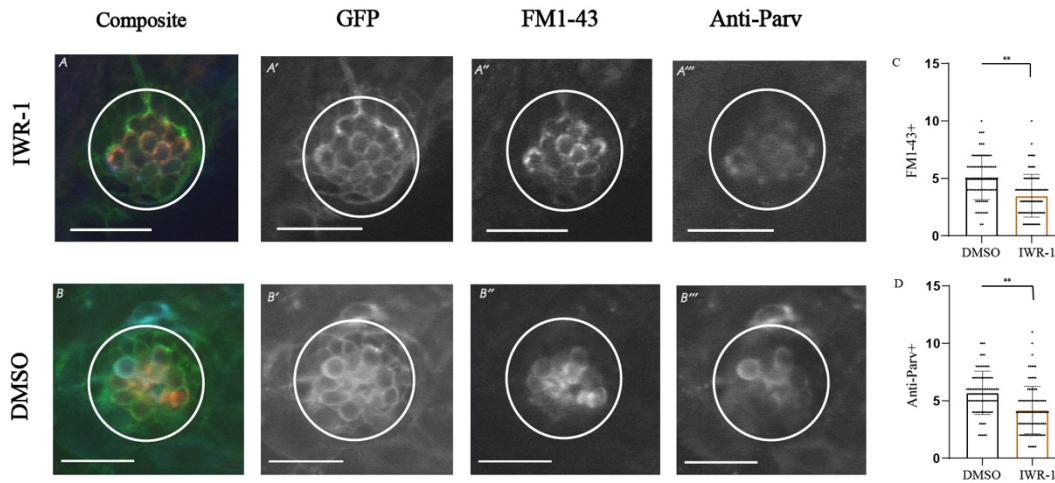


Figure 3.10 Confocal images of IWR-1 and DMSO treated fish following regeneration. Panels A-A''' are images taken of an IWR-1 treated neuromast by a confocal microscope. Panels B-B''' are images taken of an DMSO treated neuromast by a confocal microscope. The white circles highlight each neuromast. Panel C is representative of the calculated FM1-43+ averages of IWR-1 and DMSO treated neuromasts. The p-value is <0.0001. Panel D is representative of the calculated anti-parvalbumin+ averages of DMSO and IWR-1 treated neuromasts. P-value is <0.0001. The scale bar represents 20 μ m.

3.11 Proliferation in IWR-1 treated zebrafish

BrdU is a compound that incorporates into synthesizing DNA during cellular proliferation and DAPI marks the nuclei of all cells in the neuromast. Zebrafish were separated into two groups. The first was treated with IWR-1 and the second was treated with DMSO as a control. The IWR-1 treated group consisted of 5 zebrafish larvae and the DMSO treated group consisted of 14 zebrafish larvae.

The IWR-1 treated group had an average of 9.303 BrdU+ cells. The DMSO treated group had an average of 12.66 BrdU+ cells. When compared using an unpaired Student's T-test, the calculated p-value was 0.0005 (Figure 3.11). The average number of DAPI+ cells in the IWR-1 treated neuromasts was found to be 29. The average number of DAPI+ cells in the DMSO treated neuromast was 28.49. When compared using an unpaired Student's T-test, the calculated p-value was 0.7819. These results agree with previous studies showing that pharmacological inhibition of Wnt signaling results in decreased proliferation in the neuromast during regeneration. In contrast, our analysis of Wnt pathway mutants suggests a role in regulating hair cell differentiation during regeneration without a change in the level of proliferation.

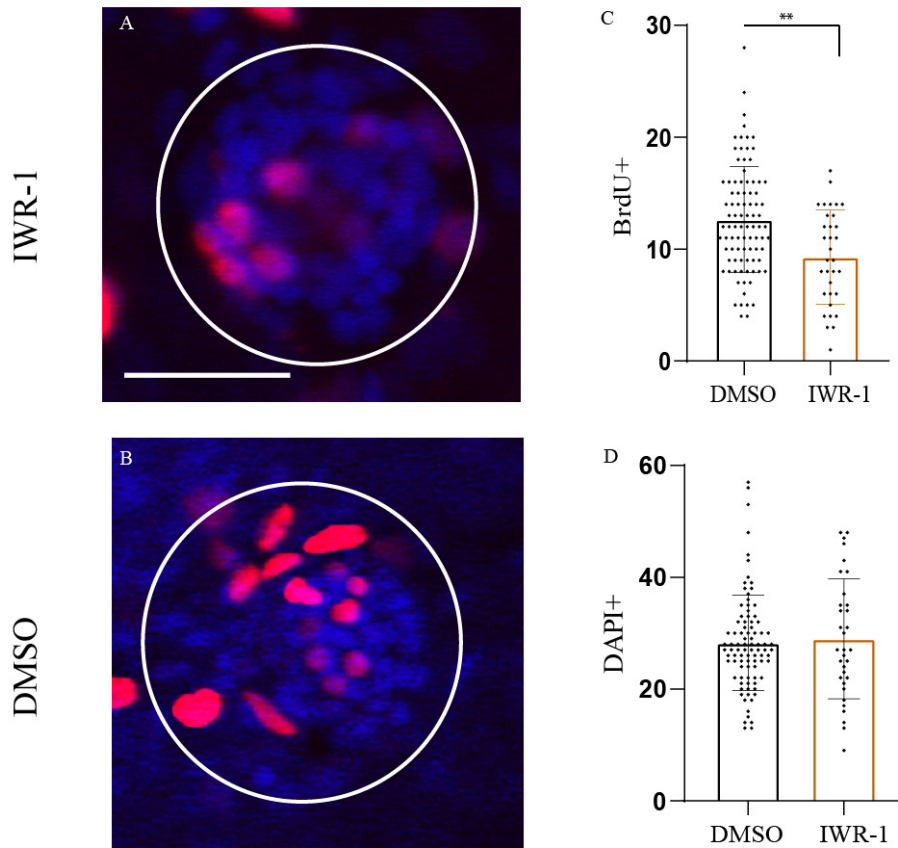


Figure 3.11 Cellular proliferation in IWR-1 and DMSO treated neuromast. Panel A is a confocal image taken of an IWR-1 treated neuromast and panel B is a confocal image of a DMSO treated neuromast. BrdU+ cells are shown in red. DAPI+ cells are shown in blue. Panel C represents the calculated averages of DMSO and IWR-1 BrdU+ cells in a neuromast. p-value is 0.0005. Panel D represents the calculated averages of DMSO and IWR-1 DAPI+ cells in a neuromast. The p-value is 0.7819. The scale bar represents 20µm.

CHAPTER 4

DISCUSSION

Within the inner ear of vertebrates reside mechanosensory hair cells that detect sound waves, which then signal to the brain. When these cells are damaged, the resulting hearing loss is irreversible. However, hair cells of similar structure and function are found along the lateral line of zebrafish. These hair cells demonstrate the robust ability to regenerate following damage (Ma et al., 2008). This makes the lateral line system an excellent model to investigate the process of hair cell regeneration.

In this study, we sought to better elucidate the involvement of the Wnt signaling pathway in lateral line hair cell regeneration. Previously, pharmacological inhibitors were used to alter Wnt signaling to study the potential role in regulating hair cell regeneration (Romero-Carvajal et al., 2015). We sought to replicate previous experiments using pharmacological agents, AZK and IWR-1, to confirm that their effects on the Wnt signaling pathway influenced the number of hair cells and proliferation in the neuromast during regeneration.

We were unable to replicate results from past research using AZK. This is an interesting find as it is possible that using this pharmacological agent is not sufficient to activate the Wnt signaling pathway during lateral line hair cell regeneration. A decrease in hair cell number and proliferation in IWR-1 supports the idea that the Wnt signaling pathway is involved in regeneration of hair cells. We sought to determine if using zebrafish lines with mutations in distinct points in the Wnt signaling pathway would give a better insight into the involvement of the pathway in lateral line hair cell regeneration.

Building upon previous research, we hypothesized that the Wnt signaling pathway is critical for hair cell regeneration in the zebrafish lateral line. Here, a novel approach was taken by using zebrafish lines that have biological mutations at distinct points along the Wnt signaling pathway. Three mutant lines were used, the first, contained a mutation for the transcription factor Lef1, second, had a null mutation of the co-receptor Kremen1 and the third was a null mutation of the receptor Lrp5.

The Wnt signaling transcription factor, Lef1, is activated when bound by β -catenin. When activated, Lef1 upregulates the transcription of downstream target genes (Daniels and Weis, 2005). We found that when Lef1 function is lost, hair cell regeneration is greatly decreased.

The decreased number of functional hair cells and total hair cells, as shown by FM1-43 and anti-parvalbumin staining, supports the hypothesis that the Wnt signaling pathway is critical for regeneration. Despite having this impact on hair cell regeneration, there was no change in cellular proliferation in the neuromasts. The lack of difference in proliferation of cells in the neuromast, but the significant difference in overall cells in the neuromast is interesting. This could suggest that Lef1 function is not involved in proliferation, but rather specification of progenitor support cells to differentiate into hair cells. Future work will investigate the role of Lef1 in regulating hair cell differentiation during regeneration using live imaging and specific marker analysis.

Kremen1 is a co-receptor for the Dkk ligand. When this ligand is bound, it causes an internalization of the Kremen1-Lrp5/6 receptor complex which is targeted for degradation (Mulvaney et al., 2016). In the zebrafish line harboring a null mutation for Kremen1, there was an increase in the overall number of hair cells and the number of functional hair cells

following regeneration. Though, there was no difference in the number of proliferating cells or the overall number of cells in the neuromast. This finding is consistent with our *lef1^{nl2}* results and suggests that the Wnt signaling pathway affects support cell differentiation into hair cells, rather than regulating proliferation.

The final mutation used in this study was a null mutation of the Wnt receptor, LRP5. In *lrp5^{nl23}* mutants, no changes in hair cell regeneration or proliferation was recorded. This finding was unexpected, as the *lrp5^{nl23}* mutants disrupts initial lateral line formation. LRP6 is a highly similar member of lipoprotein receptor-related protein family and might be acting to compensate for the loss of LRP5 function. Future work will examine the role of LRP6 in regulating hair cell regeneration. We are currently working to generate *lrp5/lrp6* double mutant lines.

Future experiments would be beneficial to expanding this study's findings. Lineage analysis experiments could be performed to compare expression of factors in lineage of support cells. Live imaging of the differentiation of support cells during regeneration in the *lef1^{nl2}*, *krm1^{nl10}* and *lrp5^{nl2}* mutants would be interesting. In the *lrp5^{nl2}* mutants, we saw no change in regeneration compared to the wildtype. This could possibly be due to overcompensation by the LRP6 receptor. It would be interesting to perform the experiments used in this study on zebrafish with a mutation in the LRP6 receptor.

This study supports the hypothesis that the Wnt signaling pathway is involved in the regeneration of lateral line hair cells in zebrafish. A novel approach to this hypothesis was taken using zebrafish with mutations at distinct points along the Wnt signaling pathway. This research will be beneficial to future studies regarding the reversal of hair cell damage in the mammalian inner ear.

REFERENCE LIST

- Amoh, Y; Hoffman, R. M. Hair follicle-associated-pluripotent (HAP) stem cells. *Cell Cycle*, **2017**, *16*, 2169-2175. doi:10.1080/15384101.2017.1356513.
- Basu, A.; Lagier, S.; Vologodskaya, M.; Fabella, B. A.; Hudspeth, A. J. (2016). Direct mechanical stimulation of tip links in hair cells through DNA tethers. *Elife*, *5*. doi:10.7554/eLife.16041
- Bleckmann, H.; Zelick, R.. Lateral line system of fish. *Integr Zool*, **2009**, *4*, 13-25. doi:10.1111/j.1749-4877.2008.00131.
- Cavanagh, B. L.; Walker, T.; Norazit, A.; Meedeniya, A. C. Thymidine analogues for tracking DNA synthesis. *Molecules*, **2009**, *16*, 7980-7993. doi:10.3390/molecules16097980.
- Chai, R.; Kuo, B.; Wang, T.; Liaw, E. J.; Xia, A.; Jan, T. A.; . . . Cheng, A. G. Wnt signaling induces proliferation of sensory precursors in the postnatal mouse cochlea. *Proc Natl Acad Sci U S A*, **2012**, *109*, 8167-8172. doi:10.1073/pnas.1202774109.
- Chazotte, B. Labeling nuclear DNA using DAPI. *Cold Spring Harb Protoc*, **2011**, *2011*, doi:10.1101/pdb.prot5556.
- Cramer, K. S.; Coffin, A. B.; Fay, R. R.; Popper, A. N. *Auditory Development and Plasticity : In Honor of Edwin W Rubel Springer Handbook of Auditory Research*; Springer international publishing: Cham, Switzerland. **2017**. doi:10.1007/978-3-319-21530-3
- Dalle Nogare, D.; Chitnis, A. B. A framework for understanding morphogenesis and migration of the zebrafish posterior Lateral Line primordium. *Mech Dev*, **2017**, *148*, 69-78. doi:10.1016/j.mod.2017.04.005.
- Dalle Nogare, D. D.; Nikaido, M.; Somers, K.; Head, J.; Piotrowski, T.; Chitnis, A. B. In toto imaging of the migrating Zebrafish lateral line primordium at single cell resolution. *Dev Biol*, **2017**, *422*, 14-23. doi:10.1016/j.ydbio.2016.12.015.
- Daniels, D. L.; Weis, W. I. Beta-catenin directly displaces Groucho/TLE repressors from Tcf/Lef in Wnt-mediated transcription activation. *Nat Struct Mol Biol*, **2005**, *12*, 364-371. doi:10.1038/nsmb912.
- Doumpas, N.; Lampart, F.; Robinson, M. D.; Lentini, A.; Nestor, C. E.; Cantu, C., Basler, K. TCF/LEF dependent and independent transcriptional regulation of Wnt/beta-catenin target genes. *EMBO J*, **2019**, *38*. doi:10.15252/embj.201798873.
- Elkon, R.; Milon, B.; Morrison, L.; Shah, M.; Vijayakumar, S.; Racherla, M.; . . . Hertzano, R. RFX transcription factors are essential for hearing in mice. *Nat Commun*, **2015**, *6*, 8549. doi:10.1038/ncomms9549.
- Estandarte, A. K.; Botchway, S.; Lynch, C.; Yusuf, M.; Robinson, I. The use of DAPI fluorescence lifetime imaging for investigating chromatin condensation in human chromosomes. *Sci Rep*, **2016**, *6*, 31417. doi:10.1038/srep31417.
- Fettiplace, R. Hair Cell Transduction, Tuning, and Synaptic Transmission in the Mammalian Cochlea. *Compr Physiol*, **2017**, *7*, 1197-1227. doi:10.1002/cphy.c160049.
- Gale, J. E.; Marcotti, W.; Kennedy, H. J.; Kros, C. J.; Richardson, G. P. FM1-43 dye behaves as a permeant blocker of the hair-cell mechanotransducer channel. *J Neurosci*, **2001**, *21*, 7013-7025.

- Ghysen, A.; Dambly-Chaudiere, C. The lateral line microcosmos. *Genes Dev*, **2007**, *21*(, 2118-2130. doi:10.1101/gad.1568407.
- Haas, P.; Gilmour, D. Chemokine signaling mediates self-organizing tissue migration in the zebrafish lateral line. *Dev Cell*, **2006**, *5*, 673-680. doi: 10.1016/j.devcel.2006.02.019.
- Harris, J. A.; Cheng, A. G.; Cunningham, L. L.; MacDonald, G.; Raible, D. W.; Rubel, E. W. Neomycin-induced hair cell death and rapid regeneration in the lateral line of zebrafish (*Danio rerio*). *J Assoc Res Otolaryngol*, **2003**, *4*, 219-234. doi:10.1007/s10162-002-3022-x.
- Heller, S.; Bell, A. M.; Denis, C. S.; Choe, Y.; Hudspeth, A. J. Parvalbumin 3 is an abundant Ca²⁺ buffer in hair cells. *J Assoc Res Otolaryngol*, **2002**, *3*, 488-498. doi:10.1007/s10162-002-2050-x.
- Hoffman, H. J.; Dobie, R. A.; Losonczy, K. G.; Themann, C. L.; & Flamme, G. A. Declining Prevalence of Hearing Loss in US Adults Aged 20 to 69 Years. *JAMA Otolaryngol Head Neck Surg*, **2017**, *143*, 274-285. doi:10.1001/jamaoto.2016.3527.
- Huelsken, J.; Behrens, J. The Wnt signalling pathway. *J Cell Sci*, **2002**, *115*, 3977-3978. doi:10.1242/jcs.00089.
- Jacques, B. E.; Montgomery, W. H. T.; Uribe, P. M.; Yatteau, A., Asuncion, J. D.; Resendiz, G.; . . . Dabdoub, A. The role of Wnt/beta-catenin signaling in proliferation and regeneration of the developing basilar papilla and lateral line. *Dev Neurobiol*, **2014**, *74*(4), 438-456. doi:10.1002/dneu.22134
- Johnson, S. L.; Safieddine, S., Mustapha, M.; Marcotti, W. Hair Cell Afferent Synapses: Function and Dysfunction. *Cold Spring Harb Perspect Med*, **2019**, *9*. doi:10.1101/cshperspect.a033175.
- Karner, C. M.; Merkel, C. E.; Dodge, M.; Ma, Z.; Lu, J.; Chen, C.;... Carroll, T.J. Tankyrase is necessary for canonical Wnt signaling during kidney development. *Dev Dyn*, **2010**, *239*(7), 2014-2023. doi:10.1002/dvdy.22340.
- Kniss, J. S.; Jiang, L.; Piotrowski, T. Insights into sensory hair cell regeneration from the zebrafish lateral line. *Curr Opin Genet Dev*, **2016**, *40*, 32-40. doi:10.1016/j.gde.2016.05.012.
- Komiya, Y.; Habas, R. Wnt signal transduction pathways. *Organogenesis*, **2008**, *4*, 68-75. doi:10.4161/org.4.2.5851.
- Kunick, C.; Lauenroth, K.; Leost, M.; Meijer, L.; Lemcke, T. 1-Azakenpallone is a selective inhibitor of glycogen synthase kinase-3 beta. *Bioorg Med Chem Lett*, **2004**, *14*(2), 413-416. doi:10.1016/j.bmcl.2003.10.062.
- Li, J.; Gong, W.; Li, X.; Wan, R.; Mo, F.; Zhang, Z.; . . . Zhao, Y. Recent Progress of Wnt Pathway Inhibitor Dickkopf-1 in Liver Cancer. *J Nanosci Nanotechnol*, **2018**, *18*, 5192-5206. doi:10.1166/jnn.2018.14636.
- Lush, M. E.; Diaz, D. C.; Koenecke, N.; Baek, S.; Boldt, H.; St Peter, M. K.; . . . Piotrowski, T. scRNA-Seq reveals distinct stem cell populations that drive hair cell regeneration after loss of Fgf and Notch signaling. *Elife*, **2019**, *8*. doi:10.7554/eLife.44431
- Ma, E. Y.; Rubel, E. W.; Raible, D. W. Notch signaling regulates the extent of hair cell regeneration in the zebrafish lateral line. *J Neurosci*, **2008**, *28*, 2261-2273. doi:10.1523/JNEUROSCI.4372-07.2008.
- MacDonald, B. T.; He, X. Frizzled and LRP5/6 receptors for Wnt/beta-catenin signaling. *Cold Spring Harb Perspect Biol*, **2012**, *4*. doi:10.1101/cshperspect.a007880.

- Matsuda, M.; Nogare, D. D.; Somers, K.; Martin, K.; Wang, C.; Chitnis, A. B. Lef1 regulates Dusp6 to influence neuromast formation and spacing in the zebrafish posterior lateral line primordium. *Development*, **2013**, *140*, 2387-2397. doi:10.1242/dev.091348.
- McGraw, H. F.; Culbertson, M. D.; Nechiporuk, A. V. Kremen1 restricts Dkk activity during posterior lateral line development in zebrafish. *Development*, **2014**, *141*(16), 3212-3221. doi:10.1242/dev.102541
- McGraw, H. F.; Drerup, C. M.; Culbertson, M. D.; Linbo, T.; Raible, D. W.; Nechiporuk, A. V. Lef1 is required for progenitor cell identity in the zebrafish lateral line primordium. *Development*, **2011**, *138*(18), 3921-3930. doi:10.1242/dev.062554
- Mulvaney, J. F.; Thompkins, C.; Noda, T.; Nishimura, K.; Sun, W. W.; Lin, S. Y., . . . Dabdoub, A. Kremen1 regulates mechanosensory hair cell development in the mammalian cochlea and the zebrafish lateral line. *Sci Rep*, **2016**, *6*, 31668. doi:10.1038/srep31668.
- Nicolson, T. The genetics of hair-cell function in zebrafish. *J Neurogenet*, **2017**, *31*, 102-112. doi:10.1080/01677063.2017.1342246.
- Niida, A.; Hiroko, T.; Kasai, M.; Furukawa, Y.; Nakamura, Y.; Suzuki, Y., . . . Akiyama, T. DKK1, a negative regulator of Wnt signaling, is a target of the beta-catenin/TCF pathway. *Oncogene*, **2004**, *23*, 8520-8526. doi:10.1038/sj.onc.1207892.
- Nixon, S. J.; Carter, A.; Wegner, J.; Ferguson, C.; Floetenmeyer, M.; Riches, J.; . . . Parton, R. G. Caveolin-1 is required for lateral line neuromast and notochord development. *J Cell Sci*, **2007**, *120*(Pt 13), 2151-2161. doi:10.1242/jcs.003830.
- Olt, J.; Johnson, S. L.; Marcotti, W. In vivo and in vitro biophysical properties of hair cells from the lateral line and inner ear of developing and adult zebrafish. *J Physiol*, **2014**, *592*, 2041-2058. doi:10.1113/jphysiol.2013.265108.
- Ornitz, D. M.; Itoh, N. The Fibroblast Growth Factor signaling pathway. *Wiley Interdiscip Rev Dev Biol*, **2015**, *4*, 215-266. doi:10.1002/wdev.176..
- Romero-Carvajal, A.; Navajas Acedo, J.; Jiang, L.; Kozlovskaja-Gumbriene, A., Alexander, R.; Li, H.; Piotrowski, T. Regeneration of Sensory Hair Cells Requires Localized Interactions between the Notch and Wnt Pathways. *Dev Cell*, **2015**, *34*, 267-282. doi:10.1016/j.devcel.2015.05.025.
- Schindelin, J.; Arganda-Carreras, I.; Frise, E.; Kaynig, V.; Longair, M.; Pietzsch, T., . . . Cardona, A. Fiji: an open-source platform for biological-image analysis. *Nat Methods*, **2012**, *9*, 676-682. doi:10.1038/nmeth.2019.
- Stamos, J. L.; Weis, W. I. The beta-catenin destruction complex. *Cold Spring Harb Perspect Biol*, **2013**, *5*, a007898. doi:10.1101/cshperspect.a007898.
- Tang, D.; He, Y.; Li, W.; Li, H. Wnt/beta-catenin interacts with the FGF pathway to promote proliferation and regenerative cell proliferation in the zebrafish lateral line neuromast. *Exp Mol Med*, **2019**, *51*, 1-16. doi:10.1038/s12276-019-0247-x.
- Thomas, E. D.; Cruz, I. A.; Hailey, D. W.; Raible, D. W. There and back again: development and regeneration of the zebrafish lateral line system. *Wiley Interdiscip Rev Dev Biol*, **2015**, *4*, 1-16. doi:10.1002/wdev.160.
- Thomas, E. D.; Raible, D. W. Distinct progenitor populations mediate regeneration in the zebrafish lateral line. *Elife*, **2019**, *8*. doi:10.7554/eLife.43736.
- Urasaki, A.; Morishita, S.; Naka, K.; Uozumi, M.; Abe, K.; Huang, L.; . . . Inagaki, N. Shootins mediate collective cell migration and organogenesis of the zebrafish

- posterior lateral line system. *Sci Rep*, **2019**, 9(1), 12156. doi:10.1038/s41598-019-48585-4
- Valdivia, L.E.; Young, R.M.; Hawkins, T.A.; Stickney, H.L.; Cavodeassi, F.; Schwarz, Q.; Pullin, L.M.; Villegas, R.; Moro, E.; Argenton, F.; Allende, M.L.; Wilson, S.W. Lef1-dependent Wnt/ β -catenin signalling drives the proliferative engine that maintains tissue homeostasis during lateral line development. *Development*, **2011**, 18, 3931-3941. doi:10.1232/dev.062695
- Voronkov, A.; Krauss, S. Wnt/beta-catenin signaling and small molecule inhibitors. *Curr Pharm Des*, **2013**, 19(4), 634-664. doi:10.2174/138161213804581837
- Xia, W.; Hu, J.; Liu, F.; Ma, J.; Sun, S.; Zhang, J.; . . . Ma, D. New role of LRP5, associated with nonsyndromic autosomal-recessive hereditary hearing loss. *Hum Mutat*, **2017**, 38, 1421-1431. doi:10.1002/humu.23285
- Yamanishi, K.; Fiedler, M.; Terawaki, S. I.; Higuchi, Y.; Bienz, M.; Shibata, N. A direct heterotypic interaction between the DIX domains of Dishevelled and Axin mediates signaling to beta-catenin. *Sci Signal*, **2019**, 12(611). doi:10.1126/scisignal.aaw5505
- Yoo, H.; Mihaila, D. M.. Neuroanatomy, Vestibular Pathways *StatPearls*. **2020**, Treasure Island (FL).
- Zhao, Y.; Yamoah, E. N.; Gillespie, P. G. Regeneration of broken tip links and restoration of mechanical transduction in hair cells. *Proc Natl Acad Sci U S A*, **1996**, 93, 15469-15474. doi:10.1073/pnas.93.26.15469

VITA

Ellen Claire Megerson was born on December 30th 1995 in Merriam, Kansas. She received a high school diploma from Shawnee Mission Northwest High School in 2014. She shortly began her college career at the University of Denver in Denver, Colorado. Her junior and senior year were spent working under John Kinnamon, PhD at the University of Denver studying the neurobiology of taste. She received a first place award for the most innovative undergraduate research at the university in 2018. She graduated with a Bachelor of Science in molecular biology and minors in chemistry and psychology. In the fall of 2018, Ellen enrolled in the graduate school at the University of Missouri-Kansas City. She joined the McGraw lab where she participated in research on the potential involvement of the Wnt signaling pathway in zebrafish lateral line hair cell regeneration.